

**T.C.
ISTANBUL AYDIN UNIVERSITY
INSTITUTE OF SCIENCE AND TECHNOLOGY**



SIGNAL PROCESSING METHOD IN GPR

THESIS

Mohammed Abdulridha ALOBAIDI

Department of Electrical & Electronic Engineering

Electrical and Electronics Engineering Program

June, 2019

**T.C.
ISTANBUL AYDIN UNIVERSITY
INSTITUTE OF SCIENCE AND TECHNOLOGY**



SIGNAL PROCESSING METHOD IN GPR

THESIS

Mohammed Abdulridha ALOBAIDI

(Y1613.300006)

**Department of Electrical & Electronic Engineering
Electrical and Electronics Engineering Program**

Advisor: Assoc. Prof. Dr. Saeid KARAMZADEH

June, 2019



T.C.
İSTANBUL AYDIN ÜNİVERSİTESİ
FEN BİLİMLER ENSTİTÜSÜ MÜDÜRLÜĞÜ

Yüksek Lisans Tez Onay Belgesi

Enstitümüz Elektrik- Elektronik Mühendisliği Ana Bilim Dalı Elektrik- Elektronik Mühendisliği (İngilizce) Tezli Yüksek Lisans Programı **Y1613.300006** numaralı öğrencisi **MOHAMMED ABDULRIDHA SAHIB AL OBAIDI'** nin "SIGNAL PROCESSING METHOD IN GPR" adlı tez çalışması Enstitümüz Yönetim Kurulunun 12.06.2019 tarih ve 2019/12 sayılı kararıyla oluşturulan jüri tarafından *aj. bilye.* ile Tezli Yüksek Lisans tezi olarak *Kor.bur.l.....* edilmiştir.

Öğretim Üyesi Adı Soyadı

İmzası

Tez Savunma Tarihi : 27/06/2019

1)Tez Danışmanı: Doç. Dr. Saeid KARAMZADEH

2) Jüri Üyesi : Dr. Öğr. Üyesi Evrim TETİK

3) Jüri Üyesi : Dr. Öğr. Üyesi Oğuz ATA

.....
[Signature]
.....
[Signature]
.....

Not: Öğrencinin Tez savunmasında **Başarılı** olması halinde bu form **imzalanacaktır**. Aksi halde geçersizdir.



DECLARATION

I hereby declare that all information in this thesis document has been obtained and presented in accordance with academic rules and ethical conduct. I also declare that, as required by these rules and conduct, I have fully cited and referenced all material and results, which are not original to this thesis.

Mohammed Abdulridha ALOBAIDI





I extend my deepest gratitude to family, whose has been a constant source of support and encouragement during all the challenges in my life.



FOREWORD

I would first like to thank my thesis advisor Assoc.Prof. Dr. Saeid KARAMZADEH of the Electric and Electronic Engineering at Istanbul Aydin University. The door to Prof. KARAMZADEH office was always open whenever I ran into a trouble spot or had a question. He consistently allowed this paper to be my own work but steered me in the right the direction whenever he thought I needed it. I would like also to thank Istanbul Aydin University and its library for providing me with an access to all the books and articles that I needed to finish this

April, 2019

Mohammed Abdulridha ALOBAIDI



TABLE OF CONTENT

	<u>Page</u>
FOREWORD	ix
TABLE OF CONTENT	xi
ABBREVIATIONS	xiii
SYMBOLS	xv
LIST OF FIGURES	xvii
LIST OF TABLES	xix
ABSTRACT	xxi
ÖZET	xxiii
1. GENERAL GPR CONCEPTS	1
1.1 Introduction	1
1.2 Objectives	3
1.3 Thesis Arrangement Layout	4
2. LITERATURE REVIEW AND THEORETICAL BACKGROUND	5
2.1 Introduction	5
2.2 Ground Penetrating Radar (GPR) Fundamentals	5
2.2.1 General	5
2.2.2 Electromagnetic wave propagation	6
2.2.3 Reflection and refraction of electromagnetic waves	6
2.2.4 Scattering attenuation	7
2.2.5 Propagation dispersion	8
2.2.6 Basic theory of GPR	8
2.2.7 Depth of penetration	11
2.2.8 Common GPR Antennas	12
2.3 Previous Studies	13
3. GPR DATA VISUALIZING AND MODELLING	17
3.1 Introduction	17
3.2 Visualizing GPR Data	17
3.2.1 A-scan	17
3.2.2 B-scan	18
3.2.3 C-scan	19
3.3 GPRMAX Simulation Program	20
3.4 GPR Systems	22
3.5 Advantages and Disadvantages of GPR	23
4. CLUTTER REDUCTION METHODS	25
4.1 Introduction	25
4.2 Background Noise and Clutter	26
4.3 Multivariate Techniques	27
4.3.1 Mean subtraction (MS)	28
4.3.2 Principal component analysis (PCA)	28
4.3.3 Independent component analysis (ICA)	29
4.3.4 Singular value decomposition (SVD)	31

4.3.5 PCA and ICA combination (PICA).....	32
4.4 FFT Analysis of GPR Signal.....	32
5. EXPERIMENTAL RESULTS	33
5.1 Introduction	33
5.2 GPR Model.....	34
5.3 Experiential Results.....	35
6. CONCLUSIONS AND RECOMMENDATIONS	41
6.1 Introduction	41
6.2 Conclusions	41
6.3 Recommendations for Future Work.....	42
REFERENCES	45
RESUME.....	51



ABBREVIATIONS

ANN	: Artificial Neural Network
A-SCAN	: One dimensional data presentation
B-SCAN	: Two dimensional data presentation
BSS	: Blind Source Separation
C-SCAN	: Three dimensional data presentation
DFT	: Discrete Fourier Transform
EM	: Electromagnetic
FFT	: Fast Fourier Transform
FT	: Fourier Transform
GPR	: Ground Penetrating Radar
ICA	: Independent Component Analysis
JADE	: Joint Approximate Diagonalization of Eigen matrices
KNN	: K-Nearest Neighbor
MMS	: Moving Median Subtraction
MS	: Mean Subtraction
NDT	: Non-Destructive Testing
PCA	: Principal Component Analysis
PICA	: Principal/ Independent Component Analysis
PRF	: Pulse Repetition Frequency
PRI	: Pulse Repetition Interval
PSNR	: Peak Signal-to-Noise Ratio
RCS	: Radar Cross Section
RF	: Radio Frequency
ROC	: Receiver Operating Characteristic
SNR	: Signal to Noise Ratio
SSIM	: Structural Similarity Index
SVD	: Singular Value Decomposition
SVM	: Support Vector Machine
UWB	: Ultra Wide-band



SYMBOLS

ω	: angular frequency
μ_x	: average of x
μ_y	: average of y
n	: column dimension
d	: depth of the reflector
D	: diagonal matrix with singular values (eigen value in diagonal matrix)
ϵ	: dielectric Permittivity
λ_{ij}	: eigen values
σ	: electrical conductivity
A_i	: transformation matrices
S_i	: subspace matrices
μ_r	: relative permibility
σ_x^2	: variance of x
σ_{xy}	: the covariance of x and y
σ_y^2	: variance of y
ϵ_r	: relative dielectric permittivity
c	: light velocity
T	: Two-way travel time to the reflector
U	: orthogonal matrix of SVD factorization
V	: orthogonal matrix of SVD factorization
d	: depth of penetration
f	: linear frequency
m	: row dimension
v	: velocity of the radar wave pulse



LIST OF FIGURES

	<u>Page</u>
Figure 1.1: GPR schematic, (from Environmental Protection Agency, Web site).	2
Figure 2.1: Many one by one signals recording by the GPR system to confirm a 2D	
Figure 2.2: Relationship of the scattering attenuation with frequency for a medium with 10 scatters per cubic meter - Each scatters has the radius 0.1 meters	7
Figure 3.1: One Dimensional GPR measurement example taken across a pipe in a box.....	18
Figure 3.2: Two-Dimensional image of GPR data for a pipe in a box at a distance of 0.4m.....	19
Figure 3.3: Three dimensional (3-D) GPR data represents an empty box.....	20
Figure 5.1: The geometrical structure of the GPR model.....	34
Figure 5.2: a GPR B-scan image.....	35
Figure 5.2:b GPR A-scan signal.....	35
Figure 5.3: The power spectrum of the GPR signal.....	35
Figure 5.4: Eigen spectra of the GPR signal.....	36
Figure 5.5.a Decluttered image using MS.....	36
Figure 5.5.b The power spectrum.....	36
Figure 5.6.a: Decluttered image using SVD.....	37
Figure 5.6.b: The power spectrum.....	37
Figure 5.7.a: Decluttered image using PCA.....	37
Figure 5.7.b: The power spectrum.....	37
Figure 5.8.a: Decluttered image of the 3 rd component using ICA.....	38
Figure 5.8.b: The power spectrum.....	38
Figure 5.9.a: Decluttered image using PICA.....	38
Figure 5.9.b: The power spectrum.....	38
Figure 5.10: The 20-ICA Eigen image components.....	39
Figure 5.11: PSNR and SSIM assessment of the multivariate removal algorithms .	40



LIST OF TABLES

	<u>Page</u>
Table 1.1: Typical parameter values including (dielectric constant, electrical conductivity, velocity and attenuation) of commonly used subsurface materials	3
Table 2.1: Typical values of radar parameters for some common materials [10].....	11
Table 2.2: Common GPR antennas	13
Table 5.1: PSNR and SSIM values for the different described clutter reduction algorithms.....	39
Table 5.2: Time performance of the different clutter reduction algorithms.....	40



SUBSPACE CLUTTER REMOVAL TECHNIQUES IN GPR

ABSTRACT

In many modern GPR systems, detecting the presence of targets, e.g, buried objects in the interference which includes clutter and noise is desired. Reflection signals obtained from hidden matters are commonly weak and blurred by vigorous clutter, which mainly comes from underground inhomogeneities, different ground surfaces natures like flat or rough kinds, and combination of connection between the transmitting and receiving antennas. Therefore, eliminating or reducing the clutter signal and unwanted noise is of essential importance.

Various signal processing techniques with multiresolution analysis like multivariate subspace-based algorithms are proposed to effectively suppress the clutter and increase the signal to the ratio of interference. The foremost includes Principal Component Analysis (PCA), Singular Value Decomposition (SVD) and Independent Component Analysis (ICA). Combining both Independent Component Analysis and Principal Component Analysis as a unique algorithm, called (PICA), has investigated and implemented. It combines the traditional PCA and ICA techniques to reduce the dimensionality by removing target uncorrelated features and hence, improve image quality and enhance their performance in image processing and GPR clutter removal tasks. PICA confirmed the ability to exclude the GPR clutter and extract or boost the target signal.

Keywords : *clutter removal; ground penetrating radar (GPR); subspace algorithms; GPRmax, multivariate techniques, PICA.*



GPR ' DE ALTUZAY KARMAŞASI GIDERME TEKNİKLERİ

ÖZET

GPR ' de Altuzay Karmaşası Giderme Teknikleri Birçok GPR sisteminde parazit ve gürültü içeren girişimlerin varlığının saptanması arzulanır. Gömülü nesnelere elde edilen yansıma sinyalleri, esas olarak yer altı homojen olmamalarından, düz veya pürüzlü zemin yüzeylerinden ve verici alıcı antenler arasında bağlantı görevi gören kuvvetli dağınıklık sebebiyle genellikle zayıf ve bulanık durumdadırlar.

Bu nedenle, dağınıklık sinyalinin ve istenmeyen gürültünün ortadan kaldırılması veya azaltılması önem arzeder. Çok değişkenli alt uzay tabanlı algoritmalar gibi çeşitli sinyal işleme teknikleri, dağınıklığı etkili bir şekilde bastırmayı hedefler ve sinyal girişim oranını artırır.

Herşeyden evvel Temel Bileşen Analizi (PCA), Tekil Değer Ayrışımı (SVD) ve Bağımsız Bileşen Analizi (ICA) içerir.

Hem bağımsız bileşen analizi hem de temel bileşen analizini benzersiz bir algoritma olarak birleştirmek (PICA olarak isimlendirilen), araştırıldı ve uygulandı. Bu da hedefle ilgili olmayan özellikleri kaldırarak boyutsallığı azaltmak, görüntü kalitesini iyileştirmek, görüntü işleme alanındaki performansı arttırmak ve GPR dağınıklığını gidermek için PCA ve ICA tekniklerini birleştiriyor. PICA, GPR dağınıklığını önüyor ve hedef sinyali çıkarma yeteneğini ortaya seriyor.

Anahtar Kelimeler : *Dağınıklık Giderme, Yer Radarı (GPR), Altuzay Algoritması, GPRmax, Çok Değişkenli Teknikler, PICA.*



1. GENERAL GPR CONCEPTS

1.1 Introduction

The Ground Penetrating Radar system (GPR) is a specific radar embedded system that is used to sense, distinguish the underground metallic and non-metallic matters, and estimate their depths and/or types such as pipes, cables, and landmines or any other dielectric material. GPR is an electromagnetic (EM) inquiry system, which is known as EM-transmission and reflection technique or shallowly surface penetrating radar.

A multiple group of service providers that incorporate engineers, archaeologists, criminologists, agronomist, environmental specialists, geologists, foresters, geophysicists, hydrologists, land use managers, and soil scientists extensively uses Ground-Penetrating Radar (GPR). In engineering applications, Non-Destructive Testing (NDT) of structures and materials including discovering suppressed structures are employed. The GPR methods sense and amount different radar waves parameters like velocity (v) and attenuation (α), and these can be used to determine the relative permittivity or dielectric constant (ϵ_r), which is the main electrical property of physical materials at various frequencies [1]. GPR devices use electromagnetic waves at high energy and frequencies (1 to 4000 MHz) to penetrate and examine the subsurface, and the radar signal propagation, which depends on the electrical properties of the ground at the high frequency [2]. GPR as a non-destructive testing technique utilizes electromagnetic radiation fields in the microwave band (VHF/UHF Frequencies) of the radio spectrum, and then detects and manipulate the reflected signals from subsurface structures. The impulse of Ground Penetrating Radar (geo-radar) as shown in Figure 1.1 is a prototype transmitting-receiving evaluating device, which processes the behavior of the reflected electromagnetic waves [3].

GPR is a geophysical tool that has become increasingly popular due to its high resolution and the need to better understand near-surface conditions [4]. In last

years, GPR has obtained admission in the search for military hazards. In many soils, excessive rates of signal attenuation slightly restrict penetration depths and limit the suitability of GPR for a huge number of applications. In salty soils, where penetration depths are generally less than 10 inches [5].

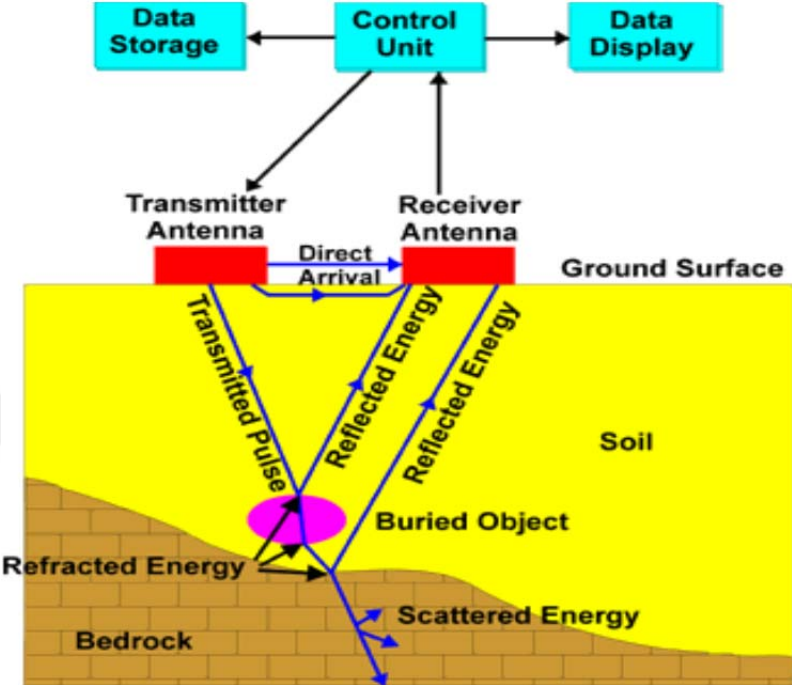


Figure 1.1: GPR schematic, (from Environmental Protection Agency, Web site).

The spread of the radar signals into earth strata relies on several electromagnetic properties of earth layers, among those, the dielectric Permittivity (ϵ) and electrical conductivity (σ) are the vital properties.

Table 1.1 lists radar parameters distinctive values of for some general materials. Velocities are mainly well lower than 0.30 mns^{-1} ($300\,000 \text{ km s}^{-1}$), the speed of light in free space. Electrical conductivity of the material at radar frequencies behaves with different manner, sometimes very considerably, from constant DC values, often increasing with frequency at roughly linear or log function of variations.

Table 1.1: Typical parameter values including (dielectric constant, electrical conductivity, velocity and attenuation) of commonly used subsurface materials [6, 7].

Material	Dielectric Constant	Electrical Conductivity (mSm ⁻¹)	Velocity (m ns ⁻¹)	Attenuation (dB m ⁻¹)
Air	1	0	0.3	0
Salt water	80	3000	0.033	600
Fresh water	80	0.5	0.033	0.1
Ice*	3-4	0.01	0.16	0.01
Granite, dry	5	0.01	0.13	0.01
Limestone*	4-8	0.5-2	0.12	0.4-1
Shales*	5-15	1-100	0.09	1-100
Sand, dry	5	0.01	0.13	0.01
Sand, wet*	20-30	0.1-1.0	0.06	0.03-0.3
Clay, wet	10	500	0.095	300
Soils:				
sandy, dry	2.6	1.4	0.19	1
sandy, wet	25	69	0.06	23
clayey, dry	2.5	2.7	0.19	3
clayey, wet	19	500	0.07	200
frozen	6	0.1	0.12	0.1

1.2 Objectives

This study aims to achieve the following:

1. Analyzing and improving the performance of GPR in detecting and characterizing non-homogeneities buried objects like pipes and cables in different environment of soil infrastructures. Significant amount of works depending on various theories in this area can be adopted.
2. Utilizing and simulating ground penetrating radar with 1.5GHz antenna frequency and studying the properties and performance of this technique for the cases under studying.
3. Proposing and comparing various signal pre-processing techniques like multivariate subspace-based algorithms to effectively suppress the clutter and increase the signal to interference ratio.
4. Detecting the presence of targets in the interference which includes clutter and noise.

The main questions to be answered were therefore if GPR measurement would stand a chance in detecting internal failure within the structure and if the provided results could of help in estimating the buildings damage or earlier life detection after exposure to an explosion or after earthquakes shock.

1.3 Thesis Arrangement Layout

The thesis is presented in six chapters:

- ❖ Chapter One: Introduces an information summary about Ground Penetration Radar, brief literature review of the previous studies that were made on, study details, aim and methodology of the study.
- ❖ Chapter Two: Provides the basic theories and concepts of the GPR, also abbreviated a review of the obtainable literature and research works, which are appertain to the present study.
- ❖ Chapter Three: Shows how to represent the GPR data in different dimensions and how to produce GPR data that can simulate the measured data.
- ❖ Chapter Four: Explains the clutter removal approaches that are suitable for the measured GPR data. Multivariate analysis techniques like PCA, ICA, SVD, and the combination are implemented and developed.
- ❖ Chapter Five: Describes the experimental program and results for the GPR data under the test. It includes the processing of data and analysis.
- ❖ Chapter Six: Presents the conclusions with general recommendation for future studies and research.

2. LITERATURE REVIEW AND THEORETICAL BACKGROUND

2.1 Introduction

This chapter handles two sections, the first one shows the GPR basics and principles, and the second part is a brief review of the realized GPR techniques for geotechnical and site investigation studies.

2.2 Ground Penetrating Radar (GPR) Fundamentals

2.2.1 General

Ground penetrating radar (GPR) is a high performance electromagnetics (EM) device or system that is aimed mainly to explore the light subsurface objects of the earth, building materials, like roads or bridges [8]. It uses microwave band (VHF/UHF Frequencies) of the radio spectrum. It emits certain electromagnetic radiation energy toward the subsurface, and identifies the reflected signals out of subsurface structures. The GPR such as impulse of Ground Penetrating Radar (geo-radar) is an embedded bidirectional transmitting-receiving evaluating device, which utilize the phenomenon of reflection of electromagnetic waves for values of the characteristics of ground layer [3] (Figure 2.1). The transmitting antenna radiates continuously tiny signal pulses with high energy-frequency (basically polarized) the radio waves into the ground. The impulses have length of twice period. The electromagnetic impulses waves propagate with radar velocity, which depends on the electromagnetic properties of penetrated material. The delay of the received waves results from the distance between the antenna of the transmitter, underground reflectors that are of low impacts, and any other materials with different electrical properties (different dielectric material) to source materials, which absorb or reflect a part of the energy of electromagnetic.

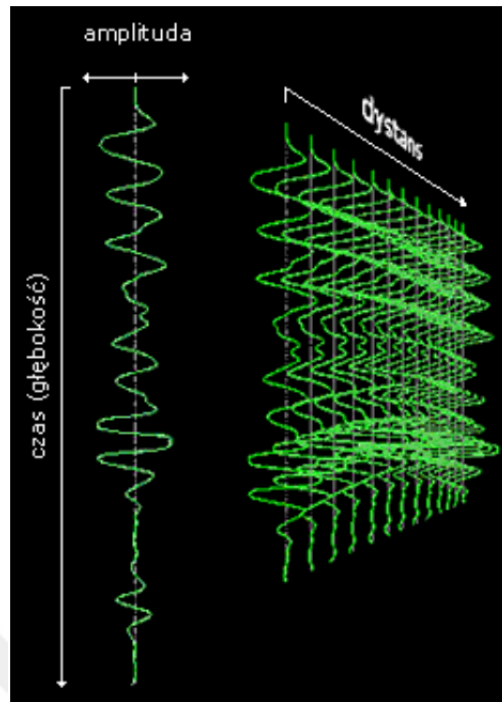


Figure 2.1: Many one by one signals recording by the GPR system to confirm a 2D (<http://GPR methodology NRCS soils>).

2.2.2 Electromagnetic wave propagation

The GPR technology uses EM-waves to investigate the subsurface. Consequently, a basic understanding of electromagnetic wave propagation phenomena is a necessary foundation to understand the method. The following brief review of the concepts is intended to establish the required background. In the following, all material properties will be treated as linear and isotropic, independent of magnitude and direction. While this is not strictly true, it is an approximation that will keep the mathematics reasonable and still, as experience shows, this gives useful results [5].

2.2.3 Reflection and refraction of electromagnetic waves

The standard GPR method uses information contained in the radiation scattered back towards the receiver by homogeneities in the ground. A brief review of the mechanisms that cause this backscattering is therefore as follows: Whenever a radar wave impinges on an object in the ground, the object reflects some of the energy and some of the energy passes through it. The waves penetrating the

object are also subject to refraction, i.e., bending of the ray paths. A wave front travelling through a medium with varying velocity changes direction according to Snell's law, originally derived for geometrical optics. When an electromagnetic wave passes through a boundary, the wave fronts must match at the interface. If the velocity is different on the two sides of the interface the direction of propagation must change so that the velocities projected on the interface are the same. In other words, the component along the interface of the propagation vector must be equal.

2.2.4 Scattering attenuation

Soil and rock generally contain randomly distributed small scale inhomogeneities that act as scatters of radar energy. For a medium with a random distribution of scatters, the effect is that for large wavelengths, a radar wave that passes through this medium is only attenuated by ohmic dissipation. As the wavelength approaches the dimension of the scatters, an increasing amount of energy is randomly scattered and less energy passes through the medium. This energy loss is said to be caused by scattering attenuation. Figure 2.2 shows an example of an estimate of the scattering attenuation. The actual values of the attenuation are not so interesting, what is important is the strong frequency dependence of this attenuation. In many cases, it is probable that it is the scattering attenuation that limits the use of high frequency antennas (www.malags.com).

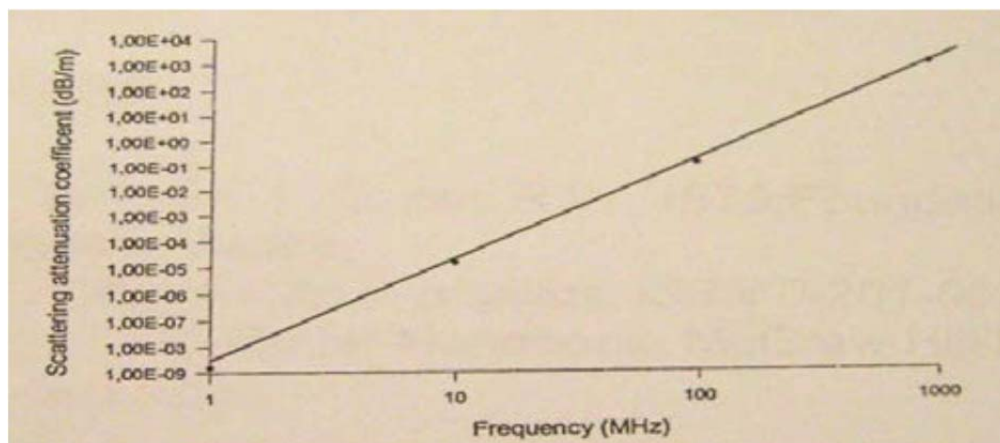


Figure 2.2: Relationship of the scattering attenuation with frequency for a medium with 10 scatters per cubic meter - Each scatters has the radius 0.1 meters (www.malags.com).

2.2.5 Propagation dispersion

Propagation dispersion is caused by the frequency dependence of the velocity and attenuation. In all physical media, both velocity and attenuation increase with frequency. For GPR application, the effect of attenuation variation is more pronounced than is the effect of velocity variation. The effect of the dispersion is that different spectral components of the pulse travel at different velocities and are attenuated at different rates. High frequency components travel faster but also decay faster. The net effect is that the pulse appears to move slower and have a lower frequency content, the longer it has travelled in the ground.

2.2.6 Basic theory of GPR

The ground penetrating radar methodology is based upon the sending of EM-pulses in the high frequency range from 1 to 4000 MHz. In this method, the travel times of the reflected waves from subsurface interfaces are noticed and recorded as they reach at the surface, and the depth (D), to an interface is derived as:

$$D = T.v/2 \quad (2.1)$$

Where:

D : depth to the reflector.

v : velocity of the radar wave pulse through the subsurface material.

T : The double -way travel time for the reflector (taken from the GPR tracer).

The ground conductivity imposes the substantial restriction on the use of radar probing, that is, the main depth to which radar wave's energy can penetrate relies on the operative conductivity of the layer being probed. This, in turn, is governed mainly by the water ability to content and its salty conditions. Moreover, the value of operational conductivity can affect directly many parameters as it is a function of density and temperature, as well as the applied frequency level of the EM-propagated waves. The penetration that occurs in saturated clayey, saline or moisture content materials is least as compared to other dry soils. Generally, the penetration depth of the electromagnetic energy in wet clay and mud mean is often less than 1meter. The commonly used technique appears to be reasonably successful in rocks and the sandy soils of the

moisture content are not saline. Rocks such as granite and limestone can be penetrated for depth of tens meters and in dry condition states, the penetration may approach 100 m [9].

GPR can combine both the transmitting and receiving antennas or use them separately. The main purpose is containing both functions. The antenna of the transmitter sends periodic interrupted sinusoidal pulses into the ground surface. When the wave hits a boundary with totally different non electric constants, i.e, (buried object), the antenna of the receiver records the variations in the reflected return signal. The principle used in reflection seismology is similar to that involved in GPRs, except that acoustic energy is used instead of EM energy, and reflections appear at boundaries with different acoustic impedances instead of dielectric constants [10].

Most of soils and rocks have potentially very low conductivity (about $< 10^{-2}$ S/m) thus the propagation of the electromagnetic waves and hence the depth of the penetration is mainly affected by electrical dielectric constant (ϵ_r) of soils and rocks under the test. The applied frequencies used are considered low compared with that of radar frequencies to ascertain their penetration inside earth layers.

Briefly, the spread of the radar signals into ground layers is a function to the electromagnetic properties of soils and rocks which are mainly electrical conductivity (σ) and dielectric permittivity (ϵ). Thus, if these properties are changed abruptly at the strata interfaces, part of the energy will be reflected as in seismic reflection. The propagation of electromagnetic (EM) waves at frequencies in the range of megahertz (radar pulse) is mainly controlled by the dielectric properties of the rock material. The radar pulse is reflected from a boundary, so that $v = 2D/T$.

The velocities of propagation of radar signal are related to the relative dielectric constant and relative permittivity (or relative non electric constant) (ϵ_r) [11]:

$$v = \frac{c}{(\mu_r \epsilon_r)^{1/2}} \quad (2.2)$$

Where $\epsilon_r = \epsilon/\epsilon_0$ is the ratio of the dielectric permittivity of the medium to the free space permittivity ($\epsilon_0=8.85*10^{-12}$ F/m), $\mu_r = \mu/\mu_0$ is the relative

permeability of the medium which is about unity for most earth soils and rocks, and ($c = 1/\sqrt{\epsilon_0\mu_0}$, $c = 3*10^8$ m/s =0.3 m/ns) is the speed of EM waves in free space. Since μ_r is close to unity for most rock materials (accept a few strongly magnetic rocks), radar velocity is primarily controlled by the dielectric constant of the medium as $\mu_r \approx 1$ [11]:

$$v = \frac{c}{(\epsilon_r)^{1/2}} \quad (2.3)$$

EM-waves rates are generally well below the 0.30 m/ns (300 000 km/s) light velocity in free space. In comparison with water for which $\epsilon_r = 81$, most geological formations have much lower values, the lowest values (in the range 3^{-10}) being dry sand/gravel and silt, unaltered hard rocks, permafrost soils and ice. The relative dielectric constant (ϵ_r) varies from 1 in air to 81 in water. Water plays an important role in the attenuation of the EM waves and it affects the GPR survey. Thus, high frequencies are used for shallow depth investigations, while low frequencies are used for large depth investigations. The depth range of GPR signals is a function to the ground electrical conductivity, the radiated power and the transmitted center frequency. The penetration depth decreases as the conductivity increases. This is because the electromagnetic energy is affected directly by the heat and much faster dissipated to heat. It may cause a huge loss in signal strength at depth. High frequencies do not penetrate as far as low frequencies, but it gives better resolution. Optimal depth penetration can be achieved in the ice where the depth of penetration may reach many hundred of meters.

Good penetration is additionally accomplished in dry sandy soils or the situation of massive dry materials such as concrete, limestone, and granite where the depth of penetration could be up to 15 meter. In clay laden and/or moist soils, saturated concrete and soils with high electrical conductivity, penetration is shallow and sometimes reaches only a few centimeters. The depth of penetration (d) is related with the electrical conductivity (σ) by the following general formula:

$$d = 35/\sigma \quad (2.4)$$

Where d is the depth of penetration in (m) and σ is the electrical conductivity in (mS/m).

2.2.7 Depth of penetration

The energy from the fields of the alternating electrical or magnetic fields produces currents that can flow in the ground. The currents that are caused in the ground may reduce the EM-waves penetration. The amount of this signal reduction is called the attenuation.

Attenuation follows an exponential law governed by an attenuation constant (α) given by [12]:

$$\alpha = \omega[\mu_a \epsilon_a \{1 + \sigma^2 / \omega^2 \epsilon_a^2\} - 1] / 2]^{1/2} \quad (2.5)$$

Where ($\omega = 2\pi f$) is the angular frequency, μ_a and ϵ_a are the entire absolute values magnetic permeability and electrical permittivity respectively, and σ is the electrical conductivity.

Table 2.1 lists some typical values of radar parameters for several common materials.

Table 2.1: Typical values of radar parameters for some common materials [10]

Material	ϵ	σ mS/m	V m/ns	α dB/m
Air	1	0	0.30	0
Ice	3–4	0.01	0.16	0.01
Fresh water	80	0.05	0.033	0.1
Salt water	80	3000	0.01	1000
Dry sand	3–5	0.01	0.15	0.01
Wet sand	20–30	0.01–1	0.06	0.03–0.3
Shales and clays	5–20	1–1000	0.08	1–100
Silts	5–30	1–100	0.07	1–100
Limestone	4–8	0.5–2.0	0.12	0.4–1
Granite	4–6	0.01–1	0.13	0.01–1
(Dry) salt	5–6	0.01–1	0.13	0.01–1

The calculations may be effortless but because GPR velocity rates are routinely quoted in mns^{-1} and frequencies in MHz, it is naive to misplace a few powers of ten unless orders of magnitude are appreciated.

The wavelength of a signal with frequency (f) is (v/f), for example signal with $f = 100 \text{ MHz}$ in air is 3 m, in rock with velocity 0.1 mns^{-1} is 10 cm.

2.2.8 Common GPR Antennas

The GPR antennas can operate in different range of frequencies. Selecting the appropriate frequency is depending on the type of working being performed, resolution, and the type of required information; one can choose low or high frequency ranges of antennas.

Wide range of frequencies from (1MHz to 4GHz) and even higher can be choice as a working frequency in the GPR systems. The operation frequency is related to the depth of penetration and hence to the attenuation (because of wave attenuation increases as the increase of depth), as well as, the type of ground (silts and clays) can limit the range of electromagnetic waves.

The electromagnetic waves with higher frequency ranges are easily and most deeply attenuated, as well as generating high frequency ranges needs to complex system. Therefore, in this case, when it is necessary to survey a deeper placed layers or objects, antennas operating at lower domain of frequencies from approximately (10 to 300) MHz are applied. However, gaining higher depths is always leads to the decrease of plumb resolution.

Low and medium frequency antennas, in the range from (1MHz to 1GHz) permit to notice larger objects, whilst high-frequency antennas, in the span from (1.5 to 4) GHz, are categorized by good resolution details and detect particular information like reinforcement bars in a concrete structure. The frequencies, depths and purposes of the common GPR antennas are illustrated as Table 2.2.

Table 2.2: Common GPR antennas

Type of antenna MHz	Depth of penetrating (m)	The Purpose (objective)
1500	0.5	Structure Evaluation
900	1.0	Structure Evaluation, Void Detection
400	4.0	Engineering, Environmental, Void Detection
200	7.0	Geotechnical, Engineering, Environmental
100	20.0	Geotechnical, Environmental, Mining

2.3 Previous Studies

Wide GPR applications related to various fields can be verified. This section is a review of the implemented GPR technique for only geotechnical and site investigation studies that are related to civil engineering.

Roddis et al. [13] applied fourteen asphalt test sections at Lawrence, U.S.A, where the pavement thickness ranged from 7.5 to 55 cm. A 73 ground truth measurements was used to calibrate the radar surveys. The study indicates that blind estimation of asphalt thickness is within 10% of actual thicknesses.

Saarenketo and Scullion [14] GPR was used in de-tecting moisture filled voids locations down a concrete structure. Because the dielectric properties of the concrete are similar to the base, in any substantial reflections in the reflected signal was related to the presence of moisture-filled voids. This study is then correlated with ground-real testing methodes. However, they were unable to distinguish between saturated layers and water filled voids.

Hunaidi and Giamou [15] used GPR for detecting leaks in buried plastic water distribution pipes. They examined the leaking of pipelines under roadway pavements in National Research Council and made a development of fiber-wrapping repair technique.

Bakir [16] used GPR method together with the electrical resistivity method for detecting the weak zones at a proposed dam site, which is located northeast of Koya city, Sulaimani. In this study 100MHz unshielded antenna was used with portable control unit. The researcher detected many anomalies like limestone rock blocks and a large zone of cavities at depth 19-28 m, the ground water table was detected too at depth 25m.

Xiujun Guo et al. [17] reported a non-destructive thickness testing of the concrete using reflection method without drilling the cores. Laboratory concrete sheets were made with varying 5~15cm according to two typical compositions. GPR system was operated with a 1.5-GHz antenna. Utilizing the reflected EM-waves with different wave velocities to determine the dielectric constant of concrete specimens. They measured the EM-waves variation to calculate concrete ages and established the dielectric model of concrete. It appears that relationship between concrete ages and dielectric constant has an exponential function.

This theory could support determining the GPR wave velocity rates allowing to the concrete age or decomposition, which could recover the detecting efficiency. This technology was successfully developed to the GPR field data composed from an investigational site in Shandong province, which proved that the relative error of this method was less than 10%.

Al-Dami [18] simulated GPR data for thin or shallow engineering experimental, detected different subsurface body groups and investigated the foundation and the investigation of the condition of re-inforced concrete by applying Ground Penetration Radar technique. The accuracy, which indicates the depth of buried bodies has very high degree of precise, but it depends on the information of the velocity of propagation of electromagnetic wave in host material that interred to the GPR device. In this study, depth of the suppressed bodies appear exactly as the same as they are placed in the hole test. The study exhibited the ability of employing the 250 MHz antenna (i.e, low frequency ranges) to explore the reinforced steel rods and their network constructions that are used in unseen able mensuration's of the building site. While, it presented the facility of using the 500 MHz antenna for identifying and investigating the subsurface re-enforced concrete in the foundation of the Plumping Units site.

Zaiyuan Zhang et al. [19] proved that GPR system can be operated to distinguish the hollow area underlying of slab pieces of the river-side slope. GPR profile obviously reveals the reflection proceedings associated to the boundary interface of the concrete slab bottom and the top of the soil surface. Herein, double-way travel time of radar wave propagated in the hollow areas is possible. The height of the hollow area derived and measured from the GPR images is almost consistent with the real data revealed by excavation on-site.

Maser et al., [20] mapped the pavement exterior thickness variations using non-electric quantities from ground penetrating signals. The air voids values was obtained from GPR-based di-electric capacities using a limit cores the number for the calibration.





3. GPR DATA VISUALIZING AND MODELLING

3.1 Introduction

GPR is a time-dependent transceiver technique that can yield good signals or images with many dimensional subsurface. It is useful for interpreting specific area and detecting targets. There are many advantages of GPR including the estimation of a precise depth for several well-known sub-surface objects. GPR has control units that produce synchronous pulses for triggering the GPR transmitter and receiver antennas.

3.2 Visualizing GPR Data

The goal of displaying the GPR data is to give a presentation of the processed data that accurately approximates an image of the subsurface with all variances that are related to the interested objects located in their appropriate spatial locations. The presentation of data is of central importance and an essential part to data interpretation.

Three display types of surface data are available including a one-dimensional (1D)

signal or trace (commonly named A-scan), a two-dimensional (2D) cross section division image (B-scan), and a three dimensional representation (3D) (nomenclature is C-scan). Since the display of surface data is a key factor to the data interpretation, the next sections discuss briefly the three forms of data presentations used in GPR to get better comprehensive thoughtful of these terminologies [21-24].

3.2.1 A-scan

A-scan is a display type of surface data as one-dimensional data appearance which illustrates a time-amplitude plot and found by a static measurement, emission, and gathering of a signal after the antenna is placing above the

position of interest. The signal gathered is displayed as signal strength vs. time delay. Figure 3.1 shows an (A-scan) plot which was taken across a pipe placed in a box.

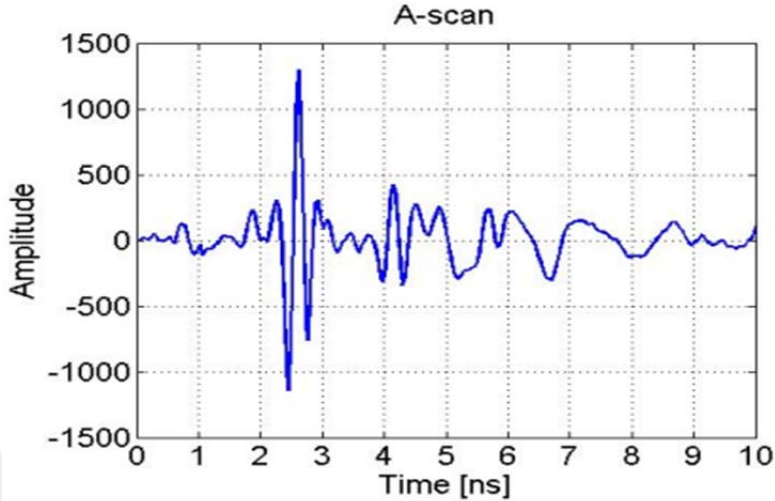


Figure 3.1: One Dimensional GPR measurement example taken across a pipe in a box

3.2.2 B-scan

B-scan (or two-dimensional data presentation) is a display type of surface data and obtained when the ensemble of A-scans is collected horizontally. In this display, the horizontal axis of the image is the surface position or distance whereas the vertical axis of the image is the round-trip time of the electromagnetic (EM) wave. Most GPR data analyses are built upon the clarification of a set of GPR signals and presented as a B-scan plot. It has two dimensions of dataset or presented as an image obtained when the ensemble of A-scans is collected horizontally. A B-scan matrix is then processed in which each entire row denotes a sample point (or time) and each column represents a trace of signal amplitude. The value of each matrix element is the voltage or current amplitude for the related trace and sample point. Attributing the intensity to the value of each matrix element allows the matrix to be showed as an image. Figure 3.2 represents B-scan of GPR data which was taken for a pipe placed in a box at 0.4 meter.

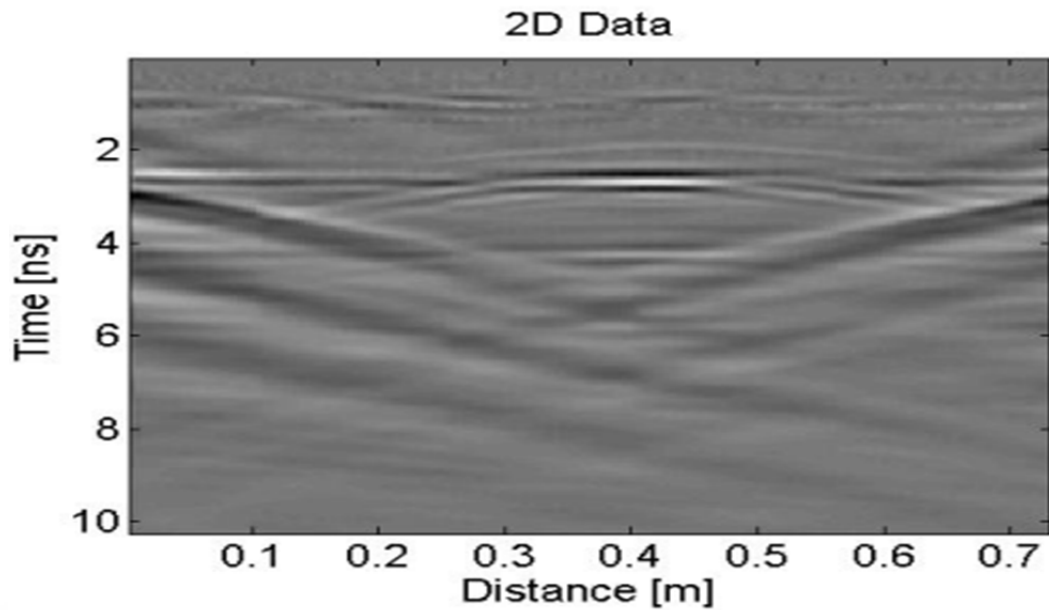


Figure 3.2: Two-Dimensional image of GPR data for a pipe in a box at a distance of 0.4m.

3.2.3 C-scan

C-scan signal is a display type that appears clearly three-dimensional data presentation. 3D GPR data is obtained when ensemble of B-scans images are simultaneously collected, it measured by several continually repeated line scans along the plane. Fundamentally, C-scan signal is a block view of GPR surface traces that are logged at different locations and places on the surface. Obtaining pure three-dimensional images is very useful for interpretation of specific targets. In three dimensional datasets, targets under studying and testing of interest are generally easier to be identified and isolated than conventional two-dimensional profile lines.

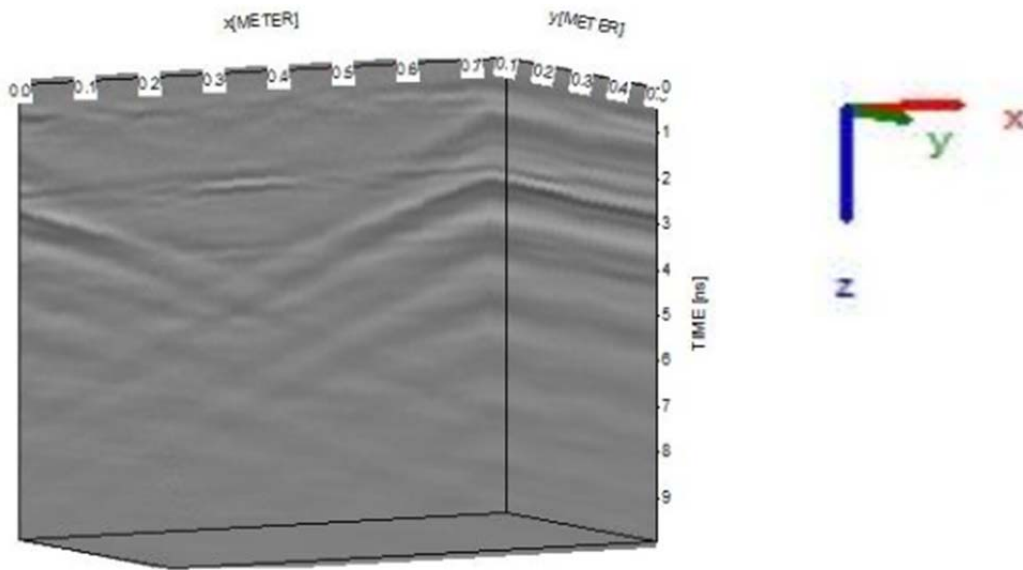


Figure 3.3: Three dimensional (3-D) GPR data represents an empty box.

3.3 GPRMAX Simulation Program

Two GPR data types (1D and 2D) was used herein to determine the performance of the completely proposed algorithms, assumed (simulated) and experimental (measured) data. GPRMax software was employed to construct the GPR data. GPRMax is an open source software used to imitate the propagation of electromagnetic (EM) wave for detection of buried object. It was first developed in 1996, the current version (version 3.1.5) was issued in 2018 and employed in this thesis for the construction of simulated dataset. Even though GPRMax was mainly designed for being used with the ground penetrating radar (GPR), it can also be adopted to imitate the propagation of electromagnetic wave in other applications. GPRMAX has been built with the Yee's algorithm in order to find the solution of the Maxwell's equation in 3D using Finite-Difference Time-Domain (FDTD) method for numerical modeling of GPR [25]. The software was written in Python and has the capability to use either CPU or GPU. Another advantage for this simulation tool includes the simple installation and upgrade process [25–27], many new features are available in the current version of the gprMax program including:

- Anisotropic material modeling

In order to accurately simulate different materials such as fiber-reinforced and wood composites, the final GPR version has the ability to specify the diagonal anisotropy of differing objects. In other words, and in opposite to isotropic material, the directions (x, y, and z) can have different values and can be defined separately.

- Dispersive material modeling

GprMax simulation software can simulate dispersive materials using the single-pole Debye model since it has a suitable common frequency range. However, this model is not enough for materials such as human tissue, water, gold, soils, and cold plasma and other functions such as multi-pole Debye, Drude and Lorentz must be used. All these functions are available in the final version of gprMax.

- Simulating of soil with realistic geometric properties and dielectric constants

The version used in this thesis can simulate different soils with more realistic geometric properties and dielectric constants. With this new feature, the dispersive material functionality is used to describe the dielectric properties of the soil.

- Building of various heterogeneous objects and soil types

With this feature, the soil dielectric properties can be described using the proposed semi-empirical model. With this model, the bulk properties of the soil such as sand particle density, sand fraction, and moisture volumetric fraction can be specified; consequently, a customize soil type can be constructed.

- The surface roughness

This feature enables the gprMax software to make different heterogeneous boxes with rough surfaces.

- Adding water or grass to surface

Water here means surface water, in this version of gprMax software, the water can be added to the surface of the soil. Moreover, the grass can be also applied to the soil surface through specifying the characteristic of blades such as number of roots and height.

- Built-in antenna models including the commercial ones

Pre-defined built-in and commercial models of antenna are also included in this gprMax software, this includes but not limited Geophysical Survey Systems, Inc. (GSSI) 1.5 GHz (Model 5100) antenna and MALA Geoscience 1.2 Ghz antenna.

- Enhanced performance for simulation

The current version of gprMax has another advantage including the ability for customization for a specific application in related to performance enhancement.

Lastly, the gprMax software has easy and very fast installation procedure in comparison to other simulation tools.

To imitate a buried object in gprMax simulation software, a script file must be written in different environment including Notepad environment. Several commands are used in the gprMax tool which can be simply divided into the following categories:

- General purpose commands
- Essential commands
- Substantial commands
- Object structuring and construction commands
- Input (source) and output (display) commands
- PML (Perfectly Matched Layer) commands

For more details, see gprMax User Guide.

3.4 GPR Systems

GPR systems can be sub-grouped based on their operating principles into four categories, which are [28]:

- Pulsed (discrete) Radar
- Stepped (progress sweep) Frequency Radar
- Pulsed Stepped Frequency Radar
- Continuous Stepped Frequency Wave Radar

3.5 Advantages and Disadvantages of GPR

In comparison to other subsurface sensing technologies and measuring devices, GPR as a site investigation and target detection purposes device has many advantages such as [23], [29-31]:

- It has a non-destructive nature;
- It has the capability to maximize the research efficacy and minimize the cost;
- It has the capability to quickly cover large areas;
- It has the ability to detect variety of metallic and non-metallic targets like metal and PVC pipes.

The geologic cross sections are often resembled by the graphical presentations of GPR data. This is another advantage since it can protect and preserve the archaeology sites where culturally sensitive features (such as human burials) are very important. Indeed, its ability to comprehensively consider a specific area in front of it, unlike other sensors that are able only to consider a direct area beneath them, affords the capacity not only to detect and identify these culturally sensitive area but also in detecting and identifying a dangerous object before the system is moving over and pasting them [31]. GPR has also the capability to elevate research efficacy by quickly conducting observations at relatively low cost in addition to covering wider areas compared to other subsurface sensing technologies. More advantage includes the easiness in pulling the antennas of GPR itself by hand or with a vehicle which can create appreciable data/unit time and consequently makes the GPR readings easier [31, 32].

Regardless all these advantages mentioned earlier, GPR possess some limitations which are [23, 30]:

- Using of it in the simulation of the heterogeneous soil can grow the possibility in obtaining more false alarms. It also has limitations in the depth of signal penetration. Therefore, a significant balance between the penetration depth and the resolution of the reflected signal is required;
- GPR device like almost electronic instruments has sensitivity to the noise or undesired signals caused by different environment factors (e.g., boulders and

tree roots), cultural factors (e.g. nearby buildings and vehicles), electromagnetic transmissions from two-way radios, cellular phones, television, and microwave equipment's. Consequently, noises on the GPR logs may be detected;

- The data gathered via GPR methods is highly subjective to the interpreting, particularly if interferences are not distinguished truly.



4. CLUTTER REDUCTION METHODS

4.1 Introduction

GPR is an embedded system that can efficiently generate and receive a certain EM wave pulses to locate, and record the type and the depth of buried objects or evaluate subsurface features that cannot be viewed visually. It is extensively used for target imaging, detection and localization, health care applications, indoor motion detection, civil engineering applications, etc [5].

It is good known that targets detection process in the GPR is greatly clutter affected. Clutter degrades the detection performance and may increase the false alarms in the non-target region, it can be caused by the intervention between the GPR transmitter and receiver antennas, replication signals from the ground which is called ground bounce and prevalence response from non-mine objects (roots, stocks, non-uniform territory and so on) [33]. Since the targets are hidden nearby the shallow surface which are involves of least metal matters, clutter overpowers target signal as amplitude of reproduced signal from the target is much weak than the ground bounce. Therefore, clutter removal techniques can increase the detection probability of the buried objects.

In GPR system, the reproduced reflected signal is composed of useful target, undesired clutter and system noise. These GPR signal components are almost under additively manner. As the system noise component has less significance compared to the other synthesis, clutter reduction approaches aim to decompose the reflected signal as target and clutter components only. There are different algorithms that can remove the clutter in the GPR images. Among those, the subspace-based methods such as principal component analysis (PCA) [34-36], independent component analysis (ICA) [37, 38], singular value decomposition (SVD) [29, 39, 40], and the possible combination between them. These techniques are based on eigen values to perform matrix decomposition on the GPR image with different constraints, after the GPR image decomposes into

multiple sub-images by these methods, the first sub-image (most dominant one) is prevailed as clutter and the remaining ones construct the target components. PCA, ICA and SVD indeed can construct multivariate subspace bases for separating the clutter from the target.

Many researches were proved that subspace-based methods are the best to obtain the ideal target shape (hyperbola) [41, 42]. They can successfully remove clutter part of the GPR image.

In addition to above clutter removal methods and in the case of rare inhomogeneous soil medium where its geometric properties vary with position along the surface, it can apply mean subtraction/removal (MS) [43], whereby the background signal can be estimated as the mean of the undesirable or untreated ensemble of GPR signals without a buried object [44]. MS approach is the simplest clutter reduction technique and is the most effective technique in an ideal situation where the ground is uniform like flat surface under the antenna path. However, for almost real soil cases, subtracting the average value may not lead to sufficient clutter reduction [45].

In this work, we've applied MS, SVD, PCA, ICA, and the combination of PCA with ICA which is called PICA methods on the B-scan GPR data. ICA based method components are reconstructed using corresponding Joint Approximate Diagonalization of Eigen matrices (JADE) [46]. GPR signals are almost of non-Gaussian distribution and above the second order moments, as a result ICA is effective to process these type of signals. Moreover, the PCA is simple and adequate for dimensionality reduction, therefore combining PCA and ICA, i.e, PICA can produce an efficient method that handles both dimensionality reduction with suitable GPR clutter removal.

4.2 Background Noise and Clutter

Background noises which are termed clutter when dealing with GPR system is well-defined as those indications that are isolated and unrelated to the objective scattering characteristics but take place in the same sample time window and have similar spectral characteristics to the objective components [5, 31]. It denotes to the point targets and small separations that mirror energy and conceal

the signals of other significant mirrored waves. The background noises are caused by separation between the antennas of the transmitter and receiver in addition to multiple reflections between the ground surface and antenna. Local variations in the ground characteristic impedance may also induce clutter along with implication of small reflection sources groups within the material. The clutter may also be caused by other close sources of electromagnetic waves, including cell phones, televisions, and transmission antennas that work in radio waves [32, 47].

The ability of GPR to detect objects is based on the input signal wavelength; hence, the image quality is improved as the wavelength decreases and the frequency increases. However, the GPR penetration of the incident wave into the soil at high frequencies may be poor whereas at low frequency, the penetration is deeper but with less resolution. Therefore, in the design of GPR system a trade-off between the penetration depth required and quality of the image must be adopted. The unique design for best image quality while ensuring enough penetration depth differs with environmental conditions, soil category, mine main features like size and position. Recently, an alternative GPR models are being developed to get optimum trade-off between the signal diffusion depth and image worth under a wide range of circumstances. Moreover, the signal-processing is considered as the most critical part in the GPR system design. In fact, this process filters out confusion clutter signals and selects the objects to be stated as the current purpose targets.

The clutters taken place in GPR systems are raised by several factors including the direct-wave arrival (this is caused by direct conjugation between transmitting and receiving antennas), ground-bounce (this is caused by reflection from the ground surface), and lastly by scattering from non-mine objects such as roots, stones, non-uniform terrain conditions and environmental factors (rain, snow etc.). These unwanted factors lower the detection precision; thus, the goal of the available clutter removal methods is to gain best accuracy.

4.3 Multivariate Techniques

The main enforcement of utilizing the multivariate techniques in GPR is usually to separate the initial data set into corresponding decomposition and

factorizations that called signal and noise subspaces in order to enhance the signal-to-noise ratio.

Similar to speech, biomedical and seismic signals, GPR is a mixtures of signals with unknown mixing coefficients. As a result, it needs to employ Blind Source Separation (BSS) [48, 49] approaches that can separate the source signals set from their mixtures signals, without knowledge needing of any information (or with very little information) about the background and sources mixture. The most BSS problems are analyzed and handled under the linear and slightly non-linear data model.

Diverse methods have been employed to find such a linear representation, including conventional methods, singular value decomposition, principal components analysis, independent component analysis, etc.

4.3.1 Mean subtraction (MS)

The subspace-based methods are non-parametric methods that can extract significant features from a mixture of data and convert the correlated mixture data variables into a set of linearly uncorrelated variables. GPR image can be represented as a matrix X with $m \times n$ dimension that includes both clutter and target signals, i.e, $X = X_{clutter} + X_{target}$. A is also an $m \times n$ transformation matrix that contains eigen vectors in decreasing order. The simplest conventional clutter removal algorithm is the mean subtraction (MS) which can be expressed as (4.1)

$$X_{ij} = A_{ij} - \text{mean}(A_{ij}) = A_{ij} - \frac{1}{n} \sum_{j=1}^n A_{ij} \quad (4.1)$$

The most basic and necessary preprocessing is to center the received signal X , i.e. make X with zero- mean variable.

4.3.2 Principal component analysis (PCA)

PCA is a simple, linear, and non-parametric method for extracting significant information from a mixture of data. PCA is employed for producing orthogonal subspaces (covariance matrix), i.e, to convert the correlated input features into useful uncorrelated features with a dimensionality reduction.

It is usually utilized in a multivariate dataset for dimensionality reduction without significant loss of information. It can precisely find the most useful variables, which are the principal components (PCs) in which the applied data can be most compactly demonstrated [50]. Amongst the purposes of employing PCA are the following [48]:

- dimensionality reduction purposes;
- solving a set of linear combinations of variables;
- selecting the discriminative features for the feature selection purposes;
- visualizing and representing of multidimensional data;
- determining the underlying variables of objects or of outliers;
- identifying the highly correlated and the uncorrelated features.

The main advantage of this technique is that, it does not require a reference signal. Firstly, covariance matrix of raw data was calculated and orthonormal matrix (A) is found using the covariance matrix of raw data. After multiplication between orthonormal matrix A and zero-mean, normalized matrix X, principal components were built.

PCA is commonly used in a variety of vigorous applications such as signal and image analysis, data visualization and pattern recognition [51, 52]. In the PCA based clutter removal method, GPR image is represented by a rectangular matrix X_{ij} with $m \times n$ dimension. After the transformation matrix A is found depending on some rules like orthogonality, it can be separated into two subspaces, target and clutter as equation (4.2):

$$X = A_1^T S_1 + \sum_{i=2}^n A_i^T S_i \quad (4.2)$$

where X is the GPR based matrix, S_i and A_i are the subspace matrices which can be decomposed and formulated according to the PCA subspace method.

4.3.3 Independent component analysis (ICA)

Unlike the PCA, which leads to uncorrelated components, ICA represents the data by statistical independent components. Moreover, ICA takes into concern the higher order moments of the statistical independence component where it is a stronger statistical property than de-correlation in PCA.

In ICA, the data components are mutually independent and of linearly distributed, also they can be mixed using an instantaneous and stationary mixing.

Several algorithms can be utilized and implemented to provide the ICA set of bases. Among those, the most known ICA algorithms are: the FastICA [53-56], Extended likelihood Infomax [57-59], Joint Approximate Diagonalization of Eigenmatrices (JADE) [60-62], and the Second Order Blind Identification (SOBI) [63-65]. In this work, we employed JADE algorithm to extract the ICA components because JADE depends on the Eigen principle, which is theoretically comparable to other multivariate approaches. As a result, it is suitable and easier to compare the results of the completely multivariate methods.

JADE algorithm performs the ICA decomposition of the given data by computing the different based eigenvalue decomposition of their cumulant tensor. The cumulant tensor eigenvalues are vectors that depict the data mixture and their independent components which corresponding to the different contributions and assistances (e.g., clutter and target). The JADE exploits the higher-order cumulants of the data combination that comprises of all higher order information of the data. The statistical dependencies among the different data components are numerically characterized with the cross-cumulants (off-diagonal elements of the cumulant matrix). If and only if all data components are statistically self-determining, the off-diagonal elements are very small and vanish (hence the resultant cumulant matrix is diagonal form).

ICA can be represented as equation (4.3)

$$X = A_1 S_1 + \sum_{i=2}^n A_i S_i \quad (4.3)$$

where X is the B-scan matrix that generated from holding the m -traces of A-scans in each entire row with k -time samples, A is an $m \times n$ basis transformation or mixing matrix, and S is the matrix that holding n -independent source signals in rows of k -traces.

In the ICA method, the output set (n -signals) is assumed that are independent with maximum likelihood estimation and minimizing mutual information where

they are originated and extracted statistically from different physical sources. In this way, ICA can manipulate or exploit the cumulative distribution function (cdf) of the source signals [66].

4.3.4 Singular value decomposition (SVD)

Recently, the Singular Value Decomposition (SVD) is considered as one of the important tools in the signal processing also at statistical data analysis. SVD decomposes the applied matrix into wide range subspace matrices with all singular values. Singular values of given data matrix contain beneficial information about the entropy, noise level, the texture, the energy, the rank of the matrix, etc.

SVD¹ matrix factorization principle can be employed in producing orthogonal subspaces and eigenvalue base matrices to solve the problem of correlated input features and to extract useful features with a dimensionality reduction [67, 68].

In the manipulation of the GPR images, SVD can provide a sufficient way for extracting algebraic features from an image [69]. A singular value decomposition of matrix X with the dimension of $m \times n$ is any function of the form:

$X = UDV^T$, where $U^{m \times m}$, $V^{n \times n}$ are mutually orthogonal matrices and $D^{m \times n}$ is a diagonal matrix with singular values arranged in descending order of magnitude $\square_{ij} = 0$ for $i \neq j$ and $\square_{ij} > 0$ for $i = j$, i.e, $D = \text{diag}(\sigma_1, \sigma_2, \dots, \sigma_n)$.

Since

$$X = UDV^T \quad (4.4)$$

$$X = \sum_{i=1}^n \sigma_i u_i v_i^T \quad (4.5)$$

$$X = X_{clutter} + X_{target} = \sigma_1 u_1 v_1^T + \sum_{i=2}^n \sigma_i u_i v_i^T \quad (4.6)$$

For equations (4.2, 4.3, and 4.6), the first part represents $X_{clutter}$, while the remaining parts are associated to X_{target} .

¹ Some useful rules of SVD are:
 $U = XX^T$, $V^T = X^T X$, $U^T U = I$, $V^T V = I$, $D = D^T \Rightarrow DD^T = D^T D = D^2$, $U^T = U^{-1}$, $V^T = V^{-1}$,
 $\text{SVD}(XX^T) = UD^2U^T$, $\text{SVD}(X^T X) = VD^2V^T$.

4.3.5 PCA and ICA combination (PICA)

Mainly, the purpose of utilizing the PCA approach is essentially to minimize the dimensionality of the applied data while ICA is to reveal the significant variables of these dataset. Because of GPR signals are normally of non-Gaussian distribution and has high order moments almost above the second order moments, needing to exploit the advantages of these two techniques (PCA and ICA) and to combine them in one technique which is called PICA. The proposed PICA is suitable for both data reduction and interpretation.

4.4 FFT Analysis of GPR Signal

Generally, GPR is a normally narrow bandwidth device. A few studies on the frequency dominant analysis of GPR signal were done on last decade [70, 71]. Until now, no effective way to quantify the GPR signal for better interpretation is clear. In order to overcome this aspect, frequency domain with Fast Fourier Transform (FFT) is attempted.

The resultant GPR signal is a form of continuous traces. Each trace is a time domain signal recorded using GPR antenna. Through applying FFT algorithm, these time domain traces are completely transformed into frequency domain indicating the frequency content of the signal. The peak frequency from FFT has nearly the same range of values for all the traces within that layer. In order to study the behavior of GPR signal on subsurface strata, GPR signal containing distinct subsurface layers is divided based on known thickness. FFT is employed to extract frequency spectrum for a few different traces (FFT magnitude vs. FFT frequency relationship). Therefore, FFT spectrum can give a good depicting about the all information of the filtered traces that were produced after applying multivariate techniques.

FFT spectral estimation technique has been confirmed as a unique and powerful tool for radar signal and image processing. Spectral estimation with FFT has been widely approved for real-time measurement due to its capability for yielding high-precision level and large classes in receiving signal and process higher-computational efficiency.

5. EXPERIMENTAL RESULTS

5.1 Introduction

The main objective of this work is to minimize or remove the clutter and other unwanted signals present in the GPR data which are not related to the target characteristics. Two robust metrics are used to the evaluation of the performance of the proposed algorithms, which are, Peak Signal-to-Noise Ratio (PSNR) and Structural Similarity Index (SSIM). They can be affectively used, as the ground-truth images are available.

SNR is the ratio of average energy of the image matrix after removing the clutter and noise to the average of matrix including clutter and noise:

$$SNR = \frac{P_{clutter\ and\ noise\ removal}}{P_{clutter\ and\ noise}} \quad (5.1)$$

SSIM indicates and assesses the similarity between the base image (reference image) and the processed image with the values between 0 and 1, where 1 represents the identical images. The SSIM index is manipulated on various windows of an image. Let, the measure between two windows x and y with

$$SSIM(x, y) = \frac{(2\mu_x\mu_y + c_1)(2\sigma_{xy} + c_2)}{(\mu_x^2 + \mu_y^2 + c_1)(\sigma_x^2 + \sigma_y^2 + c_2)} \quad (5.2)$$

where

μ_x, μ_y : the average (mean) of x and y respectively.

σ_x^2, σ_y^2 : the variance of x and y respectively.

σ_{xy} : the covariance of x and y .

c_1, c_2 : two dynamic range variables to stabilize the division over very low denominator.

5.2 GPR Model

The simulated dataset is developed by using gprMax simulation tool which has the ability of imitating real commercial antennas. For all dataset presented in this work, Geophysical Survey Systems Inc. (GSSI) 1.5 GHz (Model 5100) antenna is used. It can implement various scenarios with different objects, different soil types, and different burial depths. Therefore a huge dataset including many GPR images is easy constructed. Here, we've used gprMax to implement and study a simple and general case, which is:

- ✓ A wet sandy box with the (x,y,z) dimension (480mm, 148mm, 170mm)
- ✓ A metallic pipe which starts at (0mm, 74mm, 80mm) end at (480mm, 74mm, 80mm) coordinate along x-axis with 10mm radius.
- ✓ Antenna 5 mm upper than sandy box and 5mm distance scan.
- ✓ GSSI 1.5GHz antenna frequency.

The gprMax commands are:

Title: B-scan of a metal cylinder buried in a di-electric half-space with a GSSI 1.5GHz 'like' antenna

```
# domain: 0.480 0.148 0.235
```

```
# dx_dy_dz: 0.001 0.001 0.001
```

```
# time_window: 6e-9
```

```
# material: 3 0.001 1 0 my_sand
```

```
# box: 0 0 0 0.480 0.148 0.170 my_sand
```

```
# cylinder: 0 0.074 0.080 0.480 0.074 0.080 0.010 metallic pipe
```

Figure (5.1): depicts the geometrical structure of the case under studying.

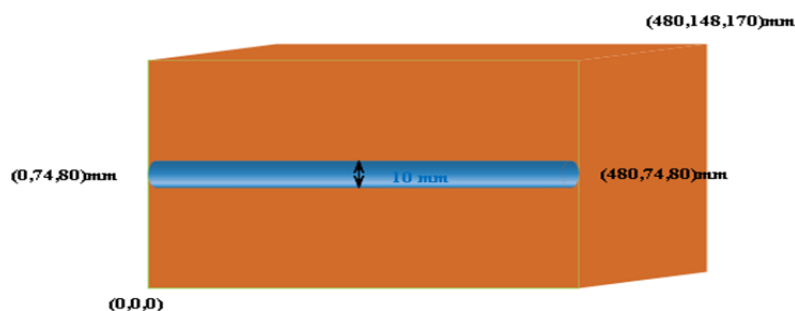


Figure 5.1: The geometrical structure of the GPR model

5.3 Experiential Results

The simulated B-scan of the GPR model is as shown in Figure 5.2.a, while the A-scan representation is as illustrated in Figure 5.2.b.

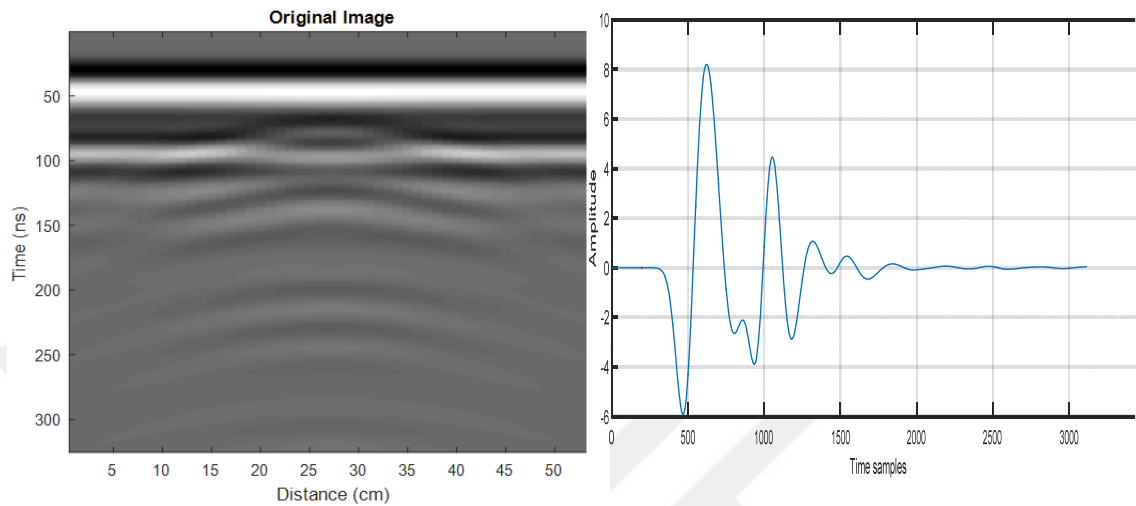


Figure 5.2: a GPR B-scan image

Figure 5.2:b GPR A-scan signal

Utilizing FFT, the power spectrum of the whole data can be estimated as shown in Figure 5.3, it is obvious that the spectrum is composed of two peaks with different amplitudes and frequencies which are corresponding to the background with the surface barrier and the PVC pipe.

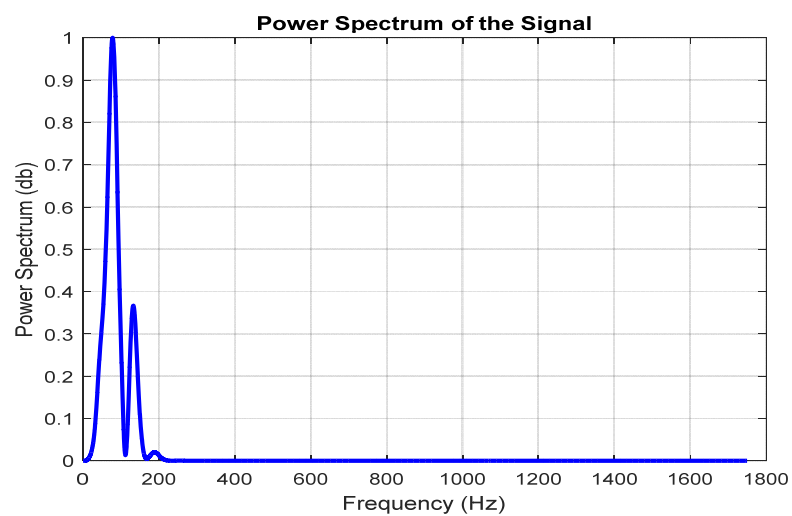


Figure 5.3: The power spectrum of the GPR signal

The GPR image data size is 325 and feature dimension is 54, i.e, 325×54 , it can exploit the principle of the eigen values and vectors to measure the appropriate feature reduction. As well as, the representation of the clutter component in GPR example is much stronger than the target section; it can be reassembled by the use of the eigen vector that corresponding to the largest eigen value of the correlation matrix of the GPR image in SVD method or the first principal component in the PCA and ICA based methods. Figure 5.4 illustrated that the most discriminative features are within the first 20 dimension, therefore it can ignore the low significant features of the GPR image and reduce the dimension of the data to 325×20 .

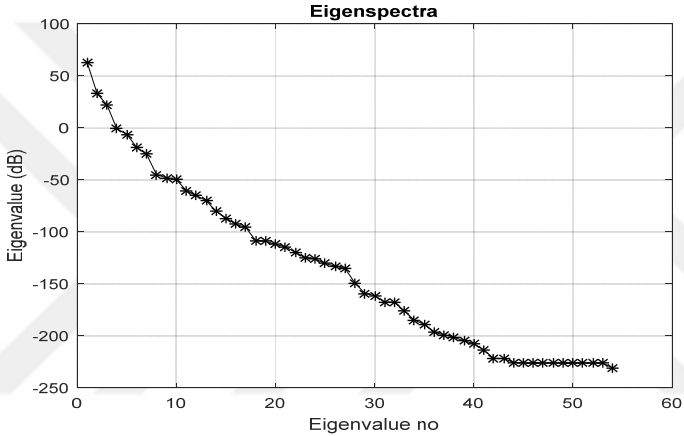


Figure 5.4: Eigen spectra of the GPR signal

Without using any prior information, the easiest clutter removal method is the mean subtraction (MS) method. Figure 5.5.a and 5.5.b explained the decluttered GPR and its corresponding power spectrum using mean subtraction method.

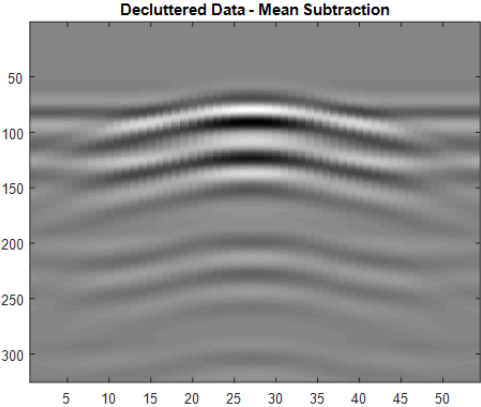


Figure 5.5.a Decluttered image using MS

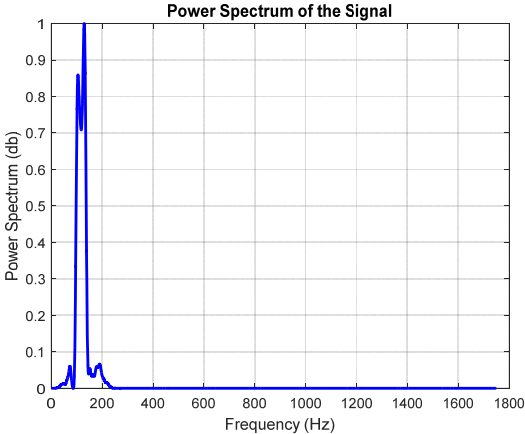


Figure 5.5.b The power spectrum

Figures (5.6-5.9) show the performance results of the SVD, PCA, 3rd principal of ICA, and the proposed PICA clutter removal methods on the real data. The signal reconstruction using 20-ICA Eigen image components is illustrated as Figure 5.10.

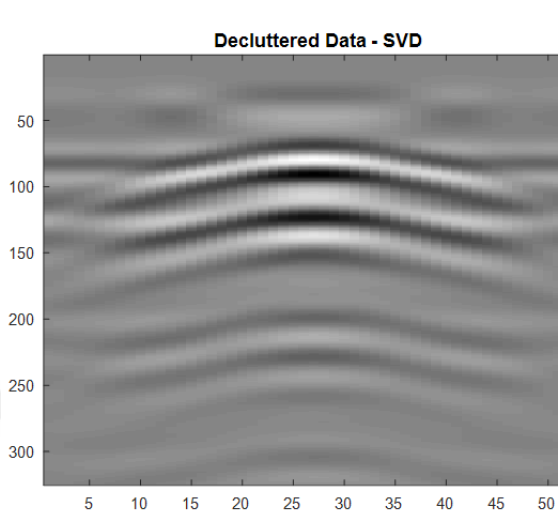


Figure 5.6.a: Decluttered image using SVD

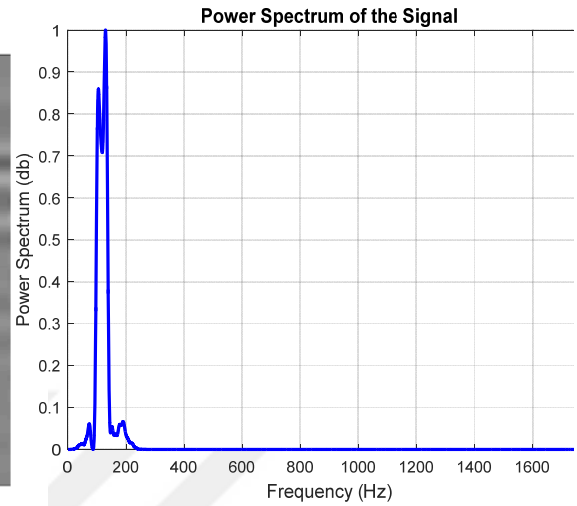


Figure 5.6.b: The power spectrum

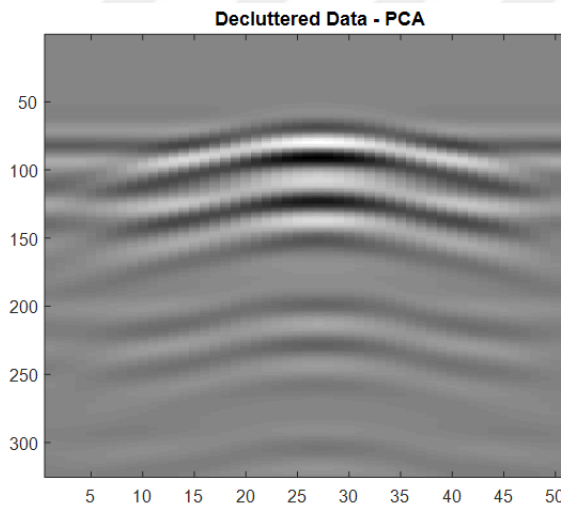


Figure 5.7.a: Decluttered image using PCA

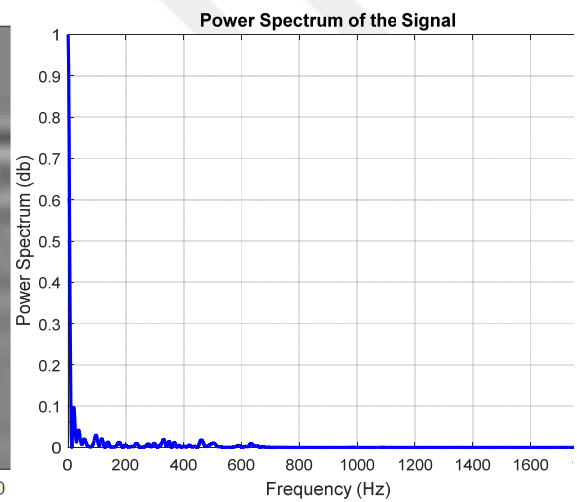


Figure 5.7.b: The power spectrum

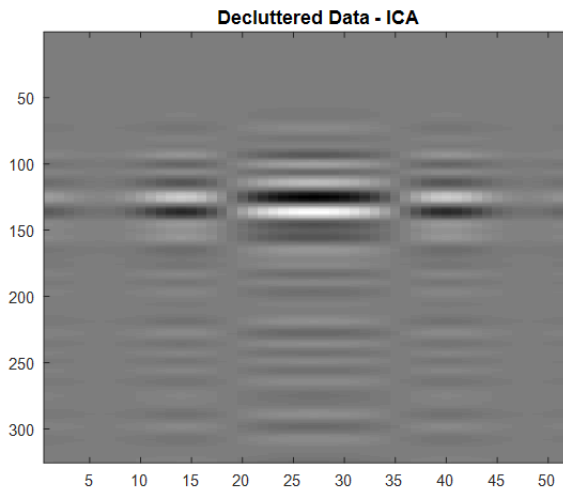


Figure 5.8.a: Decluttered image of the 3rd component using ICA

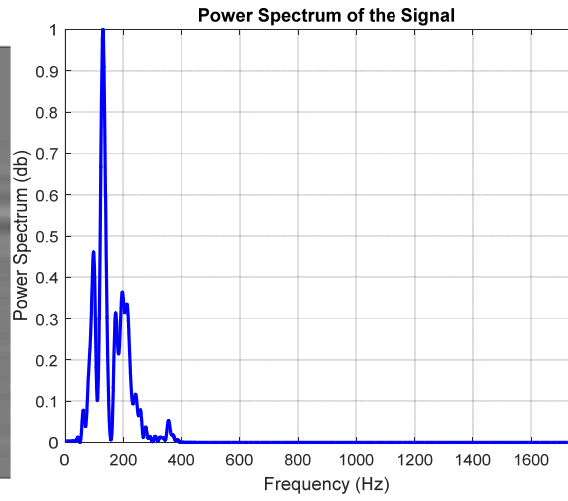


Figure 5.8.b: The power spectrum

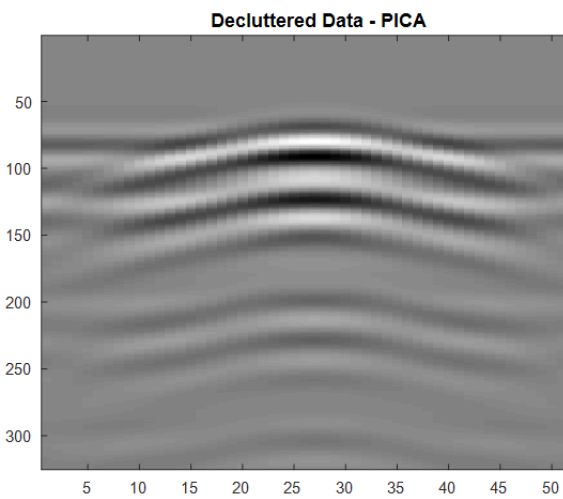


Figure 5.9.a: Decluttered image using PICA

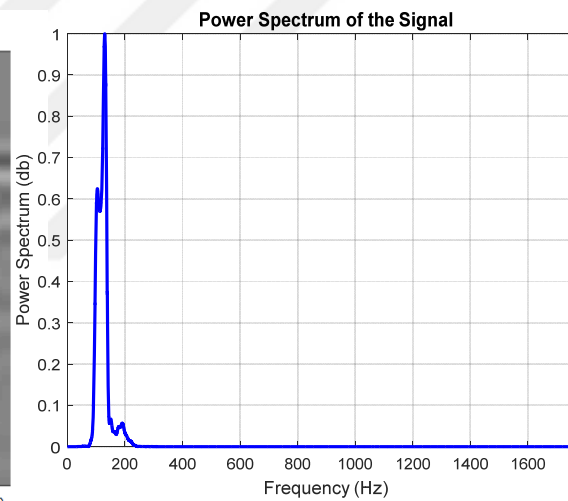


Figure 5.9.b: The power spectrum

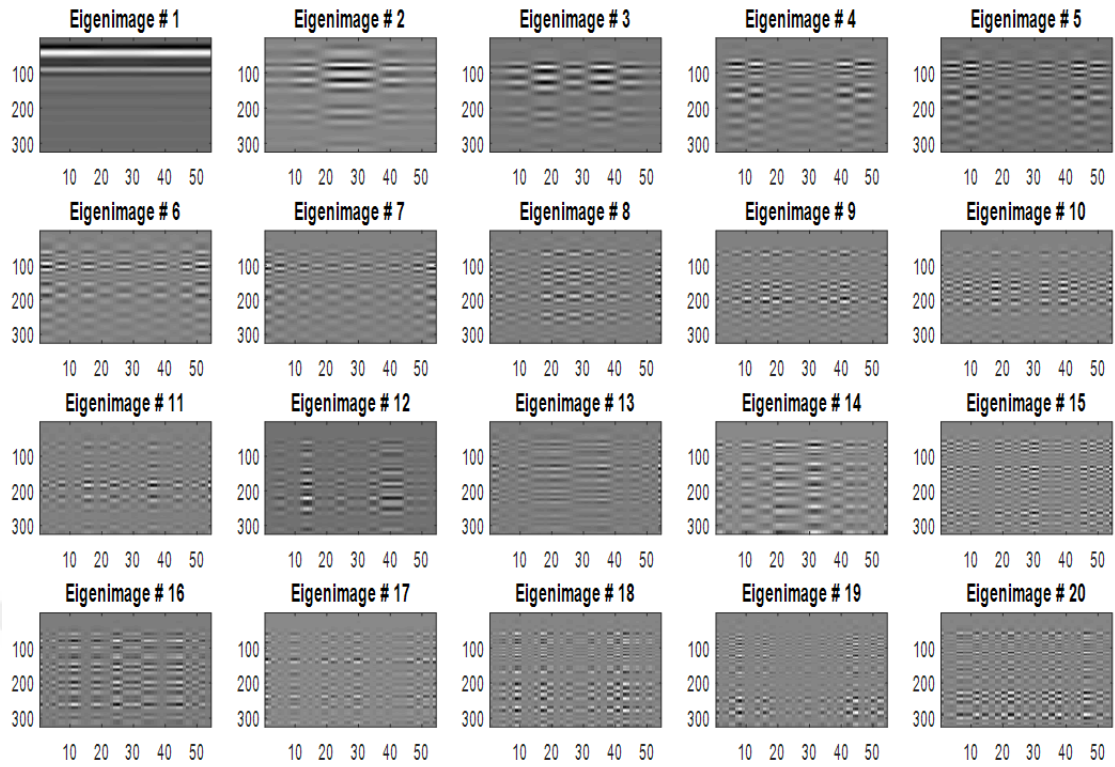


Figure 5.10: The 20-ICA Eigen image components

Table 5.1 summarizes the PSNR and SSIM performance of all decluttering techniques. Moreover, Figure 5.11 illustrates the PSNR and SSIM valuation results of the unfavorable signals multivariate removal techniques for the measured GPR data.

Table 5.1: PSNR and SSIM values for the different described clutter reduction algorithms

Algorithm	PSNR	SSIM
MS	14.632	0.22
SVD	14.712	0.35
PCA	14.344	0.28
ICA (3 rd subspace)	14.702	0.14
PICA	15.210	0.37

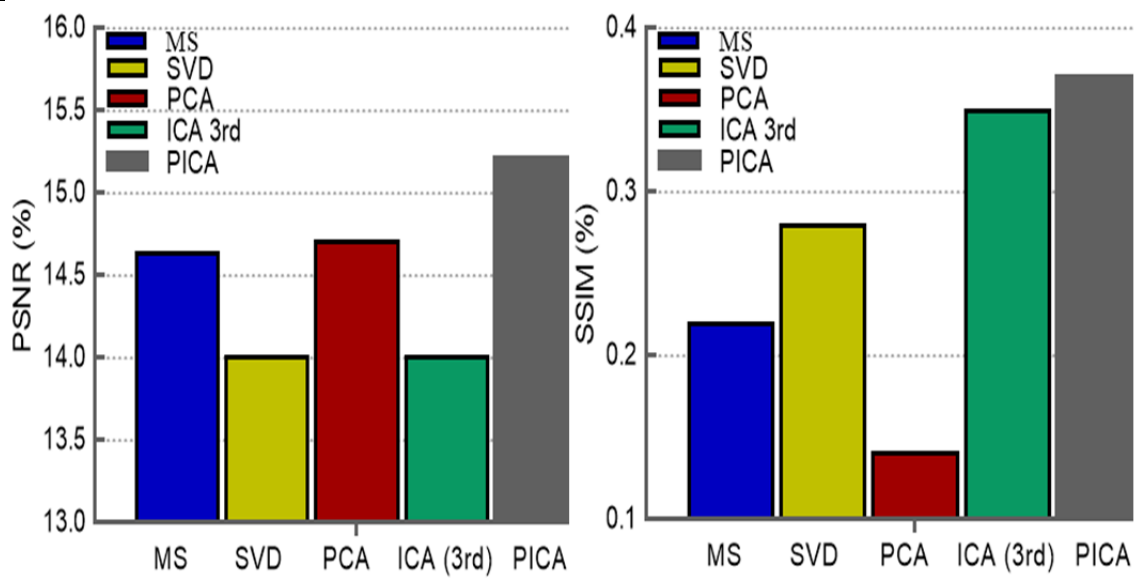


Figure 5.11: PSNR and SSIM assessment of the multivariate removal algorithms

The empirical results confirmed that the PICA approach outperforms other subspace state-of-the-art clutter removal methods.

All subspace algorithms are simulated and realized using MATLAB 8.6 (R2015b) software tool and performed on an (Intel Core i5, 2.4 GHz CPU, 4GB RAM) computer.

The running time performance of the all subspace-based GPR clutter removal algorithm is as Table 2.

Table 5.2: Time performance of the different clutter reduction algorithms

Algorithm	Time (msec)
SVD	3.73
PCA	4.10
ICA (3 rd subspace)	6.78
PICA	11.05

For all the decomposition methods, the results are satisfactory and they can remove the background and surface clutter successfully. In addition, it can reduce the dimensionality of the processed data.

6. CONCLUSIONS AND RECOMMENDATIONS

6.1 Introduction

This chapter introduces the conclusions that are obtained from the experimental results; also the recommendations for future works are presented.

Nevertheless of the GPR types and quality, almost all reflection signals directed from underground buried items into the GPR receiver antenna are usually weak and blurred by strong clutter, which mainly comes from surfaces (smooth or coarse ground), underground in-homogeneities, and non-matching between the GPR's bidirectional antennas (both the transmitter and receiver).

In this work, improving the features of GPR data in reducing the undesirable signals is significant have been introduced, and processed using simulated and measured GPR data.

6.2 Conclusions

Various well-known approaches such as mean subtraction (MS), singular value de-composition (SVD), principal component analysis (PCA), independent component analysis (ICA), and the combination (PICA) were tested and examined for the GPR clutter reduction purpose. They have been involved to the various GPR collected data with the aim to improve the data acquisition system to form good information quality by removing target uncorrelated features from the collected data and prepare reduced data for further processes like the classification tasks, which is estimated to be the next stage after clutter reduction. Consequently, the data representations handled by various feature spaces in GPR enhanced significantly the trace and object detection efficiency.

For various GPR data samples, PCA, SVD, and PICA methods are demonstrated that they are suitable for the uniform or near to uniform clutter reduction. While, for the non-uniform clutter reduction, PCA, ICA, and PICA are the

significant algorithms. These techniques can generate ideal or semi ideal data of GPR images with clutter and noise free the and enable easier detection in the next step.

The accomplished approaches were compared with GPRMAX data to assure the accuracy of the proposed techniques.

In concerning of accomplishing the objectives set of the investigations submitted in this work, it is easy to perform clutter removal for GPR systems.

6.3 Recommendations for Future Work

In light of the current study, the following points can be recommended for future studies:

- ✓ After removing the clutter and unwanted signals from the GPR data, detecting of buried objects can be implemented efficiently. It can develop robust techniques depending on the classification methods, e.g., K-Nearest Neighbor (KNN), Artificial Neural Network (ANN), Support Vector Machine (SVM), etc...
- ✓ Under the assumption of linear data model, the clutter and noise problems have been assumed and studied, where the noise-free data observations are expected to be of linear mixtures with the source signals. On the other hand a non-linear model is however likelihood, realistic and should be considered in the future.
- ✓ For achieving real Blind Source Separation (BSS), the dependences between the sources must be achieved efficiently, where correct modeling can lead to better estimation results.
- ✓ Combining other algorithms like wavelet, Hilbert, or curvelet transforms seems to be powerful and promising when applied to refresh generated raw GPR data which have not been pre-processed for clutter removal.
- ✓ Conventional FFT is limited to low frequency traces. Therefore, expanding the estimation technique to include multiple signals with high-precision can be implemented via inserting super-resolution spectral algorithm that can improve the classification and resolution capacity.

- ✓ Utilizing morphological, it can segment the Region of Interest (ROI) of the GPR image, then study and understand some physical and texture properties like occurrence, skewness or kurtosis to describe the relationship between different pixels.
- ✓ Ground penetrating radar can be used as an ultrasonic device when the area is large (as for slabs and beams), and when the ultrasonic device is not accessible, and can be used for locating voids and evaluating structure member homogeneous.
- ✓ Using multi-channelled GPR with higher frequency (e.g. 2 GHz) to promote more accurate damage monitoring data using Surfer or Tera plot software.





REFERENCES

- [1]. **Hubbard, S., Peterson, J.E., Majer, E.L., Zawislanski, P.T., Roberts, J., Williams, K.H. and Wobber, F.,** (1997), "Estimation Of Permeable Pathways and Water Content Using Tomographic Radar Data, The Leading Edge of Exploration", 16(11), 1623-1628.
- [2]. **Davis, J.L, Annan, A.P.,** (1989), "Ground penetrating radar for high- resolution mapping of soil and rock stratigraphy". Geophysical Prospecting. Vol. 37, pp. 531-551.
- [3]. **Daniels J.J.,** (2000), "Ground Penetrating Radar Fundamentals, Published Report", Department of Geological Sciences, Ohio State University, 21 pages.
- [4]. **Chen, J.,** (2001), "Bayesian Approaches for Subsurface Characterization using Hydro Geological and Geophysical Data", Ph.D. Thesis Engineering, Civil and Environmental Engineering. University of California, Berkeley.
- [5]. **Daniels, D. J.,** (2004), "Ground Penetrating Radar, 2nd Edition, The Institute of Electrical Engineers", London, United Kingdom.
- [6]. **Leckebusch J.**(2003), "Ground-penetrating radar: a modern three-dimensional prospection method". Archaeological Prospection10: 213-240.
- [7]. **Annan, A.P.,** (2001), "Ground Penetrating Radar Workshop Notes", Sensors & Software Inc.
- [8]. **Daniels J. J.,** (1996), "Surface Penetrating Radar. Radar sonar navigation and avionics series", The Institution of Electrical Engineers, London, UK.
- [9]. **Annan, A. P., and Cosway S. W.,** (1992), "Simplified GPR beam model for survey design", Society of Exploration Geophysicists, New Orleans, USA.
- [10]. **Milsom, J.,** (2003), "Filed Geophysics", third addition, University College London.
- [11]. **Rhazi M, Desbrières J, Tolaimate A, Rinaudo M, Vottero P, Alagui A.,**(2002)," Contribution to the study of the complexation of copper by chitosan and oligomers". Polymer.;43:1267–1276. doi: 10.1016/S0032-3861(01) 00685-1.
- [12]. **Charlton, M.B.,** (2008), "Principles of ground-penetrating radar for soil moisture assessment", MBCharlton.com Research Notes.
- [13]. **Roddis, W.M, Maser, K., Gisi, A.J.,**(1992),"Radar Pavement Thickness Evaluation for Varying Base Conditions, Transportation Research Record 1355.", National Academy Press, Washington D. C., pp, 90-98.
- [14]. **Saarenketo, T., and Scullion, T.,** (1994), "Ground penetrating radar applications on roads and highways," Research Report No. TX-95/1923-2F, Texas Transportation Institute, College Station.
- [15]. **Hunaidi, O., and Giamou P.,** (1998), "Ground Penetrating Radar for detection of leaks in buried plastic water distribution pipes". Seventh International Conference on Ground Penetrating Radar, Lawrence, Kansas, USA, 27-30.

- [16]. **Bakir, H. B.**, (2008), “Ground Penetration Radar and Electrical Resistivity Studies for Hamamok Dam Site”, NW Koya City, Kurdistan Region, Iraq, M. Sc. Thesis.
- [17]. **Xiujun Guo, Miao Wang , Xiaowei Zhang , Donghai Chen** ,(2011) ,” Fast non-destructive testing of concrete thicknesses using GPR”, International Conference on Remote Sensing, Environment and Transportation Engineering, Nanjing, China.
- [18]. **Al-Dami, H. A. N.**, (2011), “GPR Data Simulation for Shallow Engineering Investigations” M.Sc. thesis submitted to the Building and Construction Engineering Department of University of Technology.
- [19]. **Zaiyuan Zhang, Yonghui Zhao, Shuangcheng Ge, Poyong Sun, Chaoying Liu**, (2015), “Analysis of hollow area beneath concrete slab of seawall by means of ground penetration radar”, 8th International Workshop on Advanced Ground Penetrating Radar (IWAGPR), Florence, Italy.
- [20]. **Maser, K., and Carmicheal, A.**, (2015), “Ground Penetrating Radar Evaluation of New Pavement Density, Paving Project - SR 539 in Lynden, WA”, Final Report Submitted to Washington State Department of Transportation Research Office.
- [21]. **Brooks, J.W.**, (2000), “The Detection of Buried Non-Metallic Anti-Personnel Land Mines”, in Department of Electrical and Computer Engineering. University of Alabama: Huntsville. p. 127.
- [22]. **Belli, K.M.**, 2008, “Ground Penetrating Radar Bridge Deck Investigations Using Computational Modeling”, in College of Engineering, Department of Mechanical and Industrial Engineering. Northeastern University: Boston. p. 235.
- [23]. **Abujarad, F.**, 2007, “Ground Penetrating Radar Signal Processing For Landmine Detection”, in Institute of Electronics, Signal Processing and Communications Engineering (IESK). University of Magdeburg: Magdeburg, Germany. p. 124.
- [24]. **Huston, B., et al.**, 2002, “Nondestructive Testing of Reinforced Concrete Bridges using Radar Imaging Techniques”. Department of Mechanical Engineering, College of Engineering and Mathematics, University of Vermont: Burlington. p. 182.
- [25]. **Warren, C., Giannopoulos, A., Giannakis, I.**, (2016), “gprMax: Open source software to simulate electromagnetic wave propagation for ground penetrating radar,” Computer Physics Comm. 2209, 163-170.
- [26] **Giannopoulos, A.**, (2005), “Modelling ground penetrating radar by GprMax, Construction and building materials”, 19(10), 755–762.
- [27] **Giannakis, I., Giannopoulos, A. and Warren, C.**, (2016), “A realistic FDTD numerical modeling framework of ground penetrating radar for landmine detection”, IEEE journal of selected topics in applied earth observations and remote sensing, 9(1), 37–51.
- [28] **Pradip Kumar Mukhopadhyay**, (2005), “Three-dimensional Borehole Radar Imaging”. PhD thesis, University of Cape Town, Department of Electrical Engineering.
- [29] **Abujarad, F., G. Nadim, and A. Omar**, (2005), “Clutter Reduction and Detection of Landmine Objects in Ground Penetrating Radar Data Using Singular Value Decomposition (SVD)”. Proceedings o f the 3rd International Workshop on Advanced Ground Penetrating Radar,: p. 37-41.

- [30] **Do, J.**, (2003), "Report: Ground Penetrating Radar". Villanova University: Pennsylvania. p. 5.
- [31] **Dojack, L.**, (2012), "Ground Penetrating Radar Theory, Data Collection, Processing and Interpretation: A guide for Archaeologists", M. A. and S. Daniel, Editors. University of British Columbia: Vancouver. p. 94.
- [32] **Conyers, L.B.**, (2004), "Ground-Penetrating Radar for Archaeology", Walnut Creek, CA ; Oxford: AltaMira Press.
- [33] **Liu, J., Zhang, B. ve Wu, R.** (2006). "GPR ground bounce removal methods based on blind source separation", Progress In Electromagnetics Research Symposium, Cambridge, USA.
- [34] **Zhu, J., Xue, W., Rong, X. and Yu, Y.** (2017). "A clutter suppression method based on improved principal component selection rule for ground penetrating radar", Progress In Electromagnetics Research, 53, 29–39.
- [35] **Abujarad, F. and Omar, A.** (2006). "GPR data processing using the component-separation methods PCA and ICA, Imaging Systems and Techniques", Proceedings of the 2006 IEEE International Workshop on [Imagining read Imaging], IEEE, pp.60–64.
- [36] **Karlsen, B., Larsen, J., Sorensen, H. and Jakobsen, K.B.** (2001). Comparison of PCA and ICA based clutter reduction in GPR systems for anti-personal landmine detection, Statistical Signal Processing, 2001. Proceedings of the 11th IEEE Signal Processing Workshop on, IEEE, pp.146–149
- [37] **Karlsen, B., Sorensen, H.B., Larsen, J. and Jakobsen, K.B.** (2002). "Independent component analysis for clutter reduction in ground penetrating radar data, Detection and Remediation Technologies for Mines and Minelike Targets VII", volume4742, International Society for Optics and Photonics, pp.378–390.
- [38] **Verma, P.K., Gaikwad, A.N., Singh, D. and Nigam, M.** (2009). "Analysis of clutter reduction techniques for through wall imaging in UWB range", Progress In Electromagnetics Research, 17, 29–48.
- [39] **Cagnoli, B. and Ulrych, T.** (2001). "Singular value decomposition and wavy reflections in ground-penetrating radar images of base surge deposits", Journal of applied geophysics, 48(3), 175–182.
- [40] **Riaz, M.M. and Ghafoor, A.** (2012). Information theoretic criterion based clutter reduction for ground penetrating radar, Progress In Electromagnetics Research, 45, 147–164.
- [41] **Bostanudin, N.** (2013). "Computational methods for processing ground penetrating radar data", Ph.D. thesis, University of Portsmouth.
- [42] **Kumlu, D. and Erer, I.** (2017). "A comparative study on clutter reduction techniques in GPR images", Electrical and Electronic Engineering (ICEEE), 2017 4th International Conference on, IEEE, pp.323–328.
- [43] **Khan, U.S. and W. Al-Nuaimy.** "Background Removal from GPR Data Using Eigen values". in 13th International Conference on Ground Penetrating Radar 2010.
- [44] **Abujarad, F., A. Jostingmeier, and A.S. Omar,** "Clutter Removal for Landmine Using Different Signal Processing Techniques". Proceedings of the Tenth International Conference on Ground Penetrating Radar, Vols 1 and 2, 2004: p. 697-700.
- [45] **Van der Merwe, A. and I.J. Gupta,** "A Novel Signal Processing Technique for Clutter Reduction in GPR Measurements of Small, Shallow Land

- Mines". IEEE Transactions on Geoscience and Remote Sensing, 2000. 38(6): p. 2627-2637.
- [46] **THU Hoang, DINH-TUAN Pham, and Claudette AH-SOONL.** (2005) "Mutual information based independent component analysis of array data", <http://www.math-info.univ-paris5.fr/map5/publis/PUBLIS05/2005-17.pdf>.
- [47] **Campana, S. and S. Piro, Seeing the Unseen : Geophysics and Landscape Archaeology.** (2009), London: Taylor & Francis.
- [48] **Cichocki A. and Amari S.** "Adaptive Blind Signal and Image Processing: Learning Algorithms and Applications". John Wiley & Sons, West Sussex, UK, 2003.
- [49] **N. Thirion, J. MARS, and J. L. BOELLE.** "Separation of seismic signals: A new concept based on a blind algorithm". In Signal Processing VIII, Theories and Application, pages 85-88. Elsevier, Triest, Italy, September 1996.
- [50] **Duda, R.O., P.E. Hart, and D.G. Stork,** "Pattern Classification". 2nd. 2001, New York ; Chichester: Wiley.
- [51] **Diamantaras, K.I. and Kung, S.Y.** (1996). "Principal component neural networks: theory and applications", volume 5, Wiley New York.
- [52] **E. Oja.** "Principal components, minor components, and linear neural networks". Neural Networks, 5:927{935, 1992.
- [53] **A. Hyv̄arinen.** Fast and robust flxed-point algorithms for independent component analysis. IEEE Transactions on Neural Networks, 10(3):626{634, 1999.
- [54] **D. G. Luenberger.** Optimization by Vector Space Methods. John Wiley & Sons, 1969.
- [55] **N. Delfosse and P. Loubaton.** Adaptive blind separation of independent sources: a deflation approach. Signal Processing, 45(I):59{83, 1995.
- [56] **An xing Zhao, Yan sheng Jiang, and Wen bing Wang.** Exploring independent component analysis for GPR signal process. Progress In Electromagnetics Research Symposium, Hangzhou, China,, pages 22{26, August 2005.
- [57] **Anthony J. Bell and Terrence J. Sejnowski.** An information-maximization approach to blind separation and blind deconvolution. Neural Computation, 7(6):1129{1159, 1995.
- [58] **M. Gaeta and J.-L. Lacoume.** Source separation without prior knowledge: The maximum likelihood solution. Proc. EUSIPO, pages 621 {624, 1990.
- [59] **Pham D. T. and Garrat P.** Blind separation of mixture of independent sources through a quasi-maximum likelihood approach. IEEE Trans. on Signal Processing, 45(7):1712{1725, 1997.
- [60] **J. F. Cardoso and B. H. Laheld.** Equivariant adaptive source separation. IEEE Transactions on Signal Processing, 44(12):3017{3030, Dec 1996.
- [61] **J.F. Cardoso.** High-order contrasts for independent component analysis. Neural Computation, 11(1):157{192, 1999.
- [62] **Ch. Ziegaus and E.W. Lang.** A neural implementation of the JADE algorithm using higher-order neurons. Neurocomputing 56c, pages 79{100, 2004.

- [63] **A. Belouchrani, K. A. Meraim, J. F. Cardoso, and E. Moulines.** Second-order blind separation of correlated sources. In Proc. Int. Conference on Digital Sig. Processing, Cyprus, pages 346{351, 1993.
- [64] **A. Belouchrani, M.G. Amin, and K. Abed-Meraim.** Direction flnding in correlated noise fields based on joint block-diagonalization of spatio-temporal correlation matrices. IEEE Signal Processing Letters, 4(9), September 1997.
- [65] **A. Belouchrani, K. A. Meraim, J. F. Cardoso, and E. Moulines.** A blind source separation technique using second-order statistics. IEEE Trans. Sig. Proc., 45(2):434{444, 1997.
- [66] **James V. Stone and John Porrill.** Independent component analysis and projection pursuit: A tutorial introduction, 1998.
- [67] **Pisani D. Matrix** Decomposition Algorithms for Feature Extraction. Bioscience. (1).
- [68] **Moravec P.** Dimension Reduction Methods for Iris Recognition. CEUR Workshop Proc. 2009:80-89.
- [69] **Michael E. Wall, Andreas Rechtsteiner, and Luis M. Rocha.** Singular value decomposition and principal component analysis In: A Practical Approach to Microarray Data Analysis, chapter 5, pages 91{109. Kluwer Academic Publishers, Boston, MA, 2003.
- [70] **W. Shao, A. Bouzerdoun, S.L. Phung, B. Indraratna and C. Rujikiatkamjorn,** Automatic classification of GPR signals, 13th International Conference on Ground Penetrating Radar (2010), 1-6. USA: IEEE.
- [71] **Santos, N. Vinicius Rafael, Al-Nuaimy, Waleed, Porsani, Jorge Luis, Hirata, S. Nina Tomita, Alzubi, S.Hamzah,** Spectral analysis of ground penetrating radar signals in concrete, metallic and plastic targets, Journal of Applied Geophysics,(2013) doi: 10.1016/j.jappgeo.10.002.



RESUME



Name: MR Mohammed Abdulrdha Al-OBAIDI

Date & Place of Birth: 15/2/1991 Baghdad-Iraq

Graduation Bachelor: B.Sc. Computer Communication Engineering, Al-Mansour University College (Degree of 4th Class – Good), 30/Jun/2014.

Graduation Project:

Design and Implementing of Binary PSK (Phasing Shift Keying) using SDR (Software Defined Radio) based on FPGA(Field Programming Gate Array)

Membership of Unions:-

Iraqi Engineers Union, Degree: Assistant Reg. No. 175312 since 22-10-2014

Iraqi media organization :editor .no562 Since 1-6-2013

